University of Stavanger

Faculty of Science and Technology

MASTER'S THESIS

Study program/Specialization: Offshore Technology Marine and Subsea Technology	Spring semester, 2013 Open
Writer: Vadim A. Kutushev	..... (Writer's signature)
Faculty supervisor: Professor Ove Tobias Gudmestad External supervisors: Professor Sveinung Løset (University Centre in Svalbard) Associate Professor Alexey Viktorovich Dengaev (Gubkin Russian State University of Oil and Gas)	
Title of thesis: **Numerical simulation of ice sheet – FPSO interaction**	
Credits (ECTS): 30	
Key words: FPSO, ice sheet, level ice, moored ship, Arctic, plate theory, simulation	Pages: 65 Stavanger, 24.06.2013 Date/year

Frontpage for master thesis
Faculty of Science and Technology
Decision made by the Dean October 30th 2009

NUMERICAL SIMULATION OF ICE SHEET – FPSO INTERACTION

Kutushev, Vadim Albertovich, *master student*

Faculty of Science and Technology, University of Stavanger

ABSTRACT

The present thesis is devoted to investigation of FPSO interaction with level ice. The interaction with level ice is only addressed, disregarding other ice features. The scope of the thesis focuses upon two major problems: (1) numerical modeling of an ice sheet bending and (2) simulation of FPSO surge motion in level ice.

The consideration of an ice sheet bending is based on the thin plate theory. The problem is solved by means of finite difference method "manually" implemented in MATLAB. The numerical modeling of an ice sheet bending is intended to investigate ice failure load, which plays essential role for ship's performance in ice.

The numerical model of ice sheet bending has been tested in terms of failure mode prediction by comparison with full-scale results obtained for jacket platform in Bohai Bay, China. A satisfactory agreement of failure mode prediction has been achieved. Failure mode prediction was necessary to estimate ice breaking length. So-called "nodal analysis" concept was proposed for the purpose to determine the interaction contact width.

Two output parameters of the numerical model of ice sheet bending – ice failure load and bending failure mode – have been employed for investigation of FPSO surge motion in level ice. The simulated results of FPSO surge motion were compared with model ice tests of moored vessel behaviour in level ice and good compliance has been achieved. The numerical model has well predicted the phenomenon of mooring load increase in the case of low ice drift velocity.

The two numerical models developed within the scope of the thesis are believed to be a useful tool for investigation of ice sheet – FPSO interaction.

Acknowledgements

I would like to express my sincere gratitude to my supervisor Professor Ove Tobias Gudmestad. I am deeply grateful to him for the invaluable knowledge he gave me. I also greatly appreciate his continuous support, guidance and encouragement since the day we met. Without his help and concern this thesis would never have been possible.

I would also like to heartily thank Professor Anatoly Zolotukhin, who made our study at the University of Stavanger possible. I am also very proud that I had an opportunity to attend his brilliant lectures.

I am sincerely grateful to my co-supervisor Professor Sveinung Løset, who introduced me to the world of Arctic technology. I deeply admire his profound knowledge and high expertise, which inspired me to write my thesis on Arctic related topic.

I would also like to heartily thank my supervisor at Gubkin University Associate Professor Alexey Dengaev. I keenly appreciate our kind cooperation for more than 4 years.

I wish to express special gratitude to my parents, my brother and Guldar Minigulova. Without their support and encouragement this thesis would never have been possible.

And last, but by no means least, I thank my group mates: Boris, Christer, Joachim, Maria, Nikita, Tatiana and Timur for the great time we shared together!

TABLE OF CONTENT

LIST OF FIGURES

LIST OF TABLES

CHAPTER 1: INTRODUCTION

1.1. General

To date petroleum resources are known to be the major energy source in the world. However, conventional oil and gas fields are being depleted, while the global energy demand is increasingly growing (see Figure 1.1). As a consequence we are gradually moving towards more and more complicated and costly field developments.

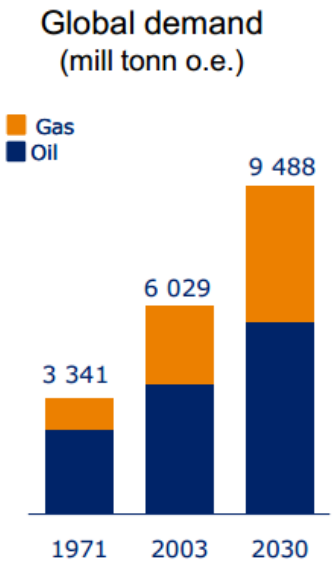

Figure 1.1: Global demand for hydrocarbon resources (Zolotukhin and Gavrilov, 2011)

Due to the fact that intensive sedimentation process has taken place in the Arctic Ocean, the region is predicted to contain large hydrocarbon resources (Zolotukhin and Gavrilov, 2011). Therefore, the interest for Arctic field developments is increasingly growing. In turn, it induces a strong requirement for investigation of ice actions on man-made structures.

The petroleum activities in the Arctic region have been begun from the exploration drilling in the Beaufort Sea since the 1970s (Garratt and Kry, 1978). Initially the offshore drilling operations were carried out from gravel artificial islands designed to withstand the impact of harsh ice environment. Then moving towards the areas with bigger water depth the requirement for fixed gravity platforms for drilling and production operations has arisen. Thus, for instance, the purpose-built mobile Arctic caisson, called Molikpaq, was deployed in the Beaufort Sea in 1984 (Hnatiuk and Felzien, 1985). At the same time, for the purposes of exploration and delineation drilling in the Beaufort Sea the innovative drillships designed to operate in harsh ice environment were employed. Initially, a fleet consisted of three ice-reinforced drillships Explorer I, Explorer II and Explorer III was deployed for drilling operations in the Beaufort Sea (Todd, 1978). Later on, conical drilling unit, named Kulluk, designed to extend drilling season has been employed (Hnatiuk and Felzien, 1985). The extension of the petroleum activities to the Arctic areas with higher water depth made the use of floating units beneficial for oil and gas production. As a consequence, two floating production storage and offloading (FPSO) units have been employed for field developments in Grand Banks, Newfoundland, in the early 2000s.

The successful experience of the operation of drillships and floating production units in ice environment has greatly influenced the interest for floaters to operate in the Arctic region. Firstly, the water depth of some Arctic areas reaches up to 3000 m (Aggarval and Souza, 2011), where production system will require the use of floating production units with subsea well completion. However, even for shallow waters, moored and thereby disconnectable structures may show to be an attractive solution in ice (Bonnemaire et al., 2007) due to possibility to avoid interaction with dangerous ice features by moving from the location. This means that the design limits for floaters can be significantly reduced compared to fixed structures (see Figure 1.2).

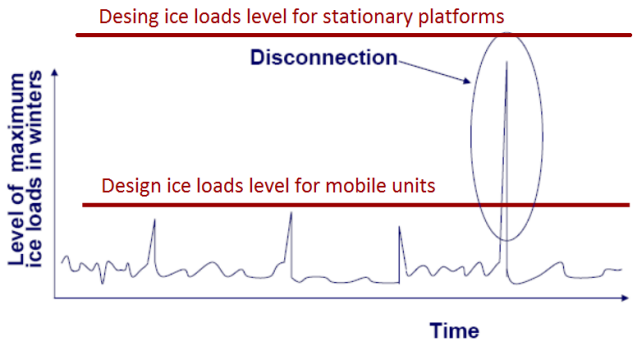

Figure 1.2: Design ice loads for stationary platforms and mobile units (Løset, 2012)

The attractiveness and in some sense the necessity of the floater operations in ice conditions triggered a tremendous effort to investigate and predict ice-vessel interaction. So far the main problems of the research are to predict vessel's behaviour in ice field, mooring loads, local ice loads, under-hull ice transport and others. With this purpose a number of model tests and numerical simulations of moored vessels' performance in ice were implemented, however, only limited full-scale data are available.

Nevertheless, behaviour of moored vessels in ice is not yet fully investigated and understood and a number of problems are still to be addressed. As an example, Aksnes (2010) (Aksnes, 2011) during experimental study of moored vessel behaviour in level ice has obtained a significant increase of mooring loads when ice drift velocity was small, which was not predicted previously by the numerical simulation. Therefore, further numerical, model and full-scale investigations of vessel's performance in ice are strongly desired.

Due to lack of full-scale data, numerical simulation of ice-vessel interaction may represent essential tool for the process investigation. Another important advantage of the numerical models is that they are not restricted to the setup parameters, contrary to the ice tank tests and full-scale studies.

1.2. Problem statement

In order to reduce ice loads on a moored vessel, implementation of an ice management is required. Therefore, the most common operational scenario for moored vessels is known to be in a broken ice field. Nevertheless, the design limits for vessels should comprise interaction with level intact ice. In addition, though ice management is implemented, the FPSO interaction with a large ice floe, which can be treated as an ice sheet, is still probable. Therefore, the thesis focuses on investigation of ice sheet – FPSO interaction.

The common design of moored vessels intended to operate in ice environment implies the turret type of mooring, which allows vessel's ice vaning. Therefore, the head-on interaction with an ice sheet is expected to be the most common scenario. This means that due to lateral confinement the vessel's surge motion when interacting with level ice is believed to be dominant. Consequently, besides other important scenarios of interaction, vessel's surge motion in level ice represents a particular problem and therefore is addressed in the thesis.

Since during head-on interaction the ice sheet normally tends to fail in bending, the horizontal loads are determined by ice failure load, i.e. the lateral load required to break an ice sheet in bending. This parameter is difficult to be determined and is usually based on empirical data. The estimations of ice failure load vary in wide range (in several times) and no strict recommendations exist. Therefore, the large emphasis of the thesis has been placed on development of a numerical tool for the purpose of estimating ice failure load.

Model tests of a moored vessel interaction with level ice have revealed that the pick mooring loads are maximum with the lowest ice drift velocity (Aksnes, 2011). Besides observed lateral confinement, this effect may be partially explained by increasing friction coefficient due to low velocity and change to static friction. To the author's knowledge, this phenomenon has not yet been taken into account by the existing numerical models. Subsequently, the numerically predicted results may appear to some extent to be underestimated in terms of peak mooring loads. Therefore, numerical investigation of the influence of dynamically changing friction coefficient on ship's performance in ice has been addressed in the thesis.

Taking the problem statement into account, the scope of the thesis is formulated in the next section.

1.3. Scope of the thesis

The objective of the present thesis is to contribute to the knowledge about FPSO operation in the Arctic environment. The thesis elaborates upon particular problem of FPSO behaviour in level ice. The scope of the thesis is further limited to in-depth investigation of FPSO surge motion during interaction with an ice sheet. For this purpose two major problems have been solved within the scope of the thesis: (1) investigation of ice failure load and (2) investigation of "locking effect" of a moored ship moving in level ice with low drift velocity due to increase of velocity-dependent friction coefficient.

To solve the first problem a numerical model of ice sheet bending based on the plate theory has been developed. The calculation procedures of the model are based on finite difference method (FDM) and "manually" implemented in MATLAB.

For the purpose of solving the second problem a numerical model of moored vessel's surge motion in level ice has been developed. The model is mainly based on the ideas of an icebreaker performance in level ice.

CHAPTER 2: OVERVIEW OF FPSO OPERATIONS IN ICE ENVIRONMENT

2.1. Experience of FPSO operation at Terra Nova field

The general aspects of Terra Nova field development are described in the paper of Lever et al (2000). The Terra Nova oil field is located in the Jeanne D'Arc basin approximately 350 km east of St. John's, Newfoundland. The water depth of the area is 90-100 m. The location of the Terra Nova field's area is shown in Figure 2.1.

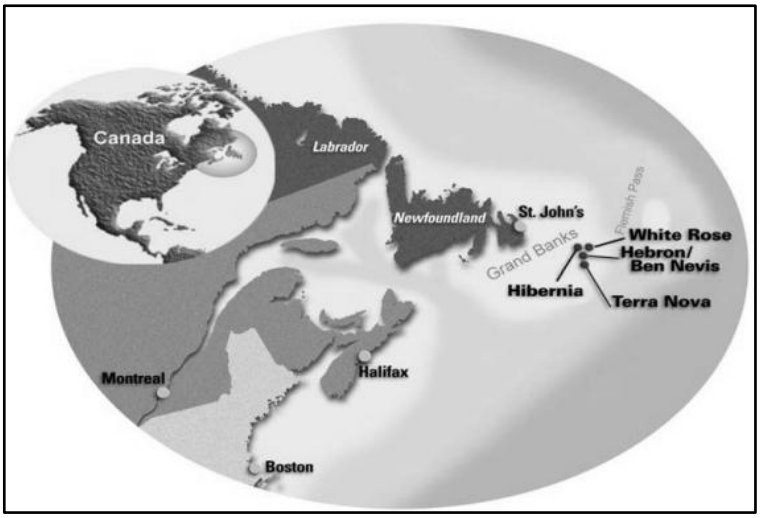

Figure 2.1: Grand Banks area location (Norman et al, 2008)

As can be seen from Figure 2.1 the area is characterized by wide petroleum production activities and includes several producing fields – Terra Nova, White Rose, Hibernia and Hebron. Two of these fields are being developed utilizing FPSO units, namely Terra Nova and White Rose oil fields. The White Rose project will be briefly described in the next section.

The peculiarity of the Terra Nova field development consists in harsh environmental conditions of the area of location. The main environmental challenges of the FPSO operation at the Terra Nova field are (Lever et al., 2000):

- Low air and water temperatures;
- Fog;
- Sea ice and icebergs;
- Extreme currents, waves and wind.

Table 2.1 provides a summary of the design environmental conditions at Terra Nova.

Table 2.1: Environmental criteria at Terra Nova (Duggal et al 2009)

Parameter	1-Year	100-Year	Units
Waves, Hs	10.9	16	m
Waves, Tp	12.9 - 16.0	15.7 - 20.2	sec
Wind, Vw	28.8	39.6	m/s
Current, Vc	1	1.3	m/s
Pack Ice	0 - 30	> 50 - 70	% coverage
Icebergs	<100,000	>100,000	MT

Here we will consider only ice related attributes of FPSO operation at Terra Nova, since it is only relevant to the current work. The ice conditions at Terra Nova area are characterized by both pack ice and icebergs (Gudmestad et al., 2007).

Pack ice at Terra Nova is represented by first-year ice with mean period of intrusion of about 40 days every three years (Lever et al., 2000). Lever et al. (2000) state that the mean coverage of the broken ice field is estimated to be approximately $3/10^{th}$ with the maximum value of $9/10^{th}$ cover. The thickness of the ice ranges between 0.3 and 1.5 metres.

Pack ice is quite challenging for vessel's operation since it creates an additional load to the hull and the mooring system. Since pack ice can damage the vessel's hull, the hull has to be ice-strengthened. Mooring lines and mooring system at a ship have to be designed to withstand loads exerted by ice action and to provide appropriate station-keeping. An additional concern of pack ice presence is that it can create ice accumulation near the hull. Such rubble piles exert bigger loads than distributed pack ice. Another significant problem of moored ship operation in a broken ice is complicated whether- (and ice-) vaning. In some cases different directions of water, ice and wind actions occur, and in such situations pack ice can cause significant problem by preventing a vessel to change its heading to reduce loads. It should also be mentioned that the presence of pack ice significantly worsens logistics, impeding supply vessels to operate in the area. Gudmestad et al. (2007) state that combined fog and ice at Terra Nova produces some of the most challenging navigable waters in the world.

However, for the Terra Nova field iceberg impact situations are considered to be more critical than pack ice presence (Gudmestad et al. 2007). Grand Banks region is characterized by waters significantly infested by icebergs. At Terra Nova location within 1^{o} square centered at the field the mean number of sited icebergs is 32, with the maximum value being 283 (Lever et al., 2000). The icebergs presented in the region vary widely in mass, reaching more than 1,500,000 tonnes. Figure 2.2 provides iceberg mass distribution in the region.

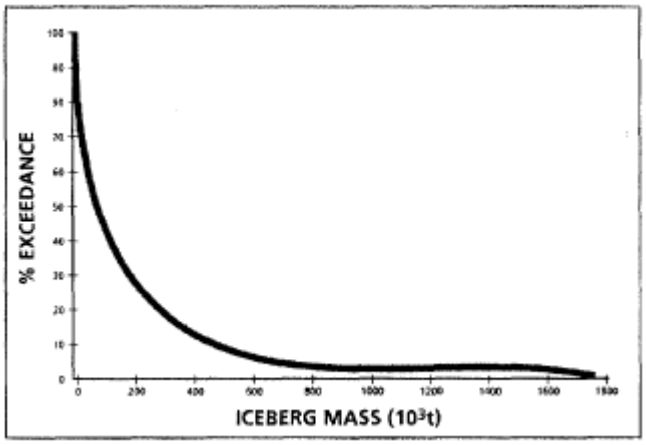

Figure 2.2. Grand Banks iceberg mass distribution (Lever et al., 2000)

Due to the huge mass of icebergs and the fact that they may have high velocity (up to several m/sec), the icebergs' impact with a vessel is considered to be very dangerous. Firstly, the hull of a ship can be damaged due to collision with an iceberg. Another key problem is again severe loads on the mooring system. Risers and mooring lines are exposed to the risk as well. Besides the risks connected with iceberg-vessel interaction, for shallow waters there is a big danger of subsea equipment damage due to iceberg gouging.

In order to design FPSO for such severe ice environment numerical simulations and ice tank tests were carried out (Duggal et al., 2009). This testing was intended to investigate FPSO behaviour in pack ice conditions, associated loads, to select appropriate mooring system, disconnection system and to choose the effective strategy of ice management. The results of the numerical and model investigations showed that the selected mooring system successfully handles loads from the pack ice and even unbroken level ice (see Figure 2.3).

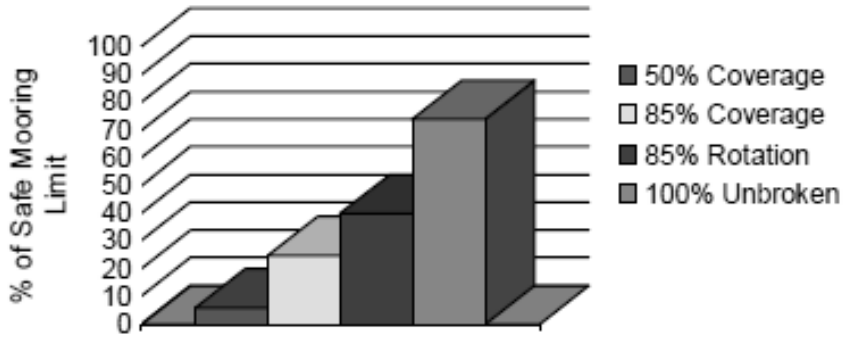

Figure 2.3. Results of model testing of pack-ice loads on FPSO (Duggal et al., 2009)

Basing on the technical requirements and on the results of numerical simulation and ice basin tests, the unique design of FPSO was chosen for operation in such challenging environmental conditions. Firstly, the hull of the FPSO was ice-strengthened for the case of iceberg impact and interaction with pack ice. The hull was reinforced by 3,000 tonnes of steel, which allowed FPSO to withstand an impact with an iceberg of 100,000 tonnes at velocity of 0.5 m/sec or with a bergy bit of mass 2,800 tonnes at velocity of 5 m/sec (Lever et al., 2000).

Big waves and currents in combination with pack ice conditions necessitated the mooring system design to be of turret type. Such system allows changing of heading and provides

significant reduction of exerted loads. The important design issue was the optimum location of the turret that provides ease vaning in pack ice. Another attribute of the FPSO's station keeping system is the use of Thruster Assisted Position Mooring System (TAMPS), which includes five azimuth thrusters and nine mooring lines fixed on anchor piles at the seabed (Gudmestad et al., 2007).

The main advantage of floaters compared to fixed platforms (as e.g. Hibernia GBS platform installed at the same region) in presence of big icebergs is their disconnection and moving off the position possibility. With regard to this, Terra Nova FPSO was equipped with unique turret mooring system with quick automated disconnection possibility. In compliance with technical requirements the FPSO was designed to disconnect in a controlled manner within 4 hours and to provide emergency disconnection in 15 minutes in the case of an undetected iceberg (Duggal et al., 2009).

So far the Terra Nova oil field is successfully producing utilizing FPSO. According to Duggal et al. (2009), ice management at the field well copes with existing ice conditions. Supply tugs successfully tow all approaching icebergs with the risk of impact. So far pack ice did not exert such loads that would necessitate FPSO disconnection. In situations of severe pack ice action, ice management vessels efficiently assisted, breaking ice to smaller floes and preventing huge ice accumulation near the hull. According to Duggal et al. (2009), up until the date of his article (8 years of the Terra Nova FPSO operation) the FPSO has performed well in this harsh environment and has been disconnected only once for FPSO upgrades and repair without incident.

Thus, FPSO at Terra Nova pioneered oil production by means of a floating unit in ice environment and by its successful experience inspired use of FPSO further, as at the adjacent oil field White Rose.

2.2. Experience of the SeaRose FPSO operation at White Rose field

The White Rose project is particularly described in the paper of Norman et al. (2008). The White Rose field development is the second project utilizing FPSO in the ice conditions. The White Rose oil field is located in Grand Banks, Eastern Canada, about 350 km East of St. John's, Newfoundland and Labrador (see **Figure 2.1**). The water depth of the field's location is approximately 120 m.

The environmental conditions of the area are almost the same as for the Terra Nova field that were briefly described in the previous section. The only difference in the environment is stated by Gudmestad et al. (2007). Since the White Rose field's location is closer to the main body of the Labrador Current than those of Terra Nova and Hibernia, sea ice and icebergs can quickly be driven into the area, which necessitates the ice management to be even more alert.

FPSO for the White Rose oilfield (SeaRose FPSO) is designed with regard to lessons learned during operation of Terra Nova FPSO. The SeaRose FPSO is imposed to almost the same technical requirements as for Terra Nova and includes the same principal features, namely turret mooring system, quick connection/disconnection (QC/DC) possibility and reinforced hull to withstand ice loads. Noticeable difference in the principle design features is that her turret system is not thruster assisted and has no powered rotation (only "pure weathervaning")

(Norman et al., 2008). The summary of the main parameters of FPSOs at Terra Nova and White Rose is presented in Table 2.2.

Table 2.2. Main parameters of Terra Nova and SeaRose FPSOs.

	Terra Nova FPSO	***SeaRose FPSO***
Length, [m]	292.2	267
Length between perpendiculars, [m]	277	256
Breadth of hull, [m]	45.5	46
Depth of hull, [m]	28.2	26.6
Designed draught, [m]	12.77 – 18.55	18
Displacement, [tonne]	194,000 (at max draught)	187,100
Liquid cargo capacity, [m^3]	151,400	148,200
Hull features	Double skin hull, ice-strengthened	Double skin hull, ice-strengthened
Designed iceberg impact resistance, [tonnes]	100,000	100,000
Mooring type	Turret	Turret
Number of mooring lines	9 (3x3 @ 120^o)	9 (3x3 @ 120^o)
Mooring lines arrangement	see Figure 2.4	see Figure 2.5
Mooring system thruster assistance	Yes (TAMPS system)	No
Planned disconnection time, [hours]	4-6	4
Emergency disconnection time, [min]	20	15

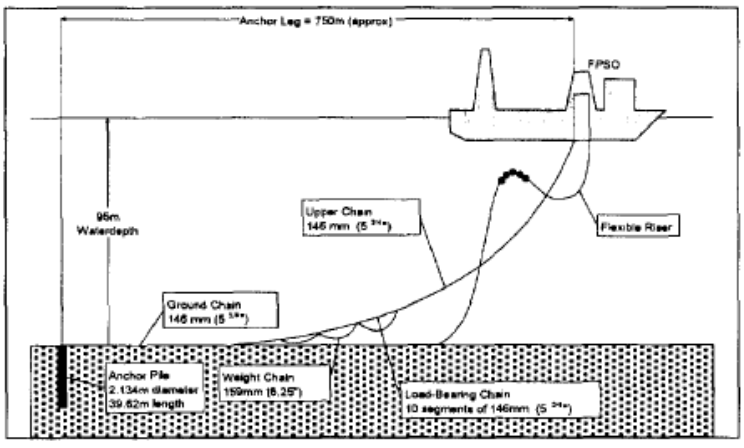

Figure 2.4. Mooring lines arrangement at Terra Nova (Lever et al., 2000)

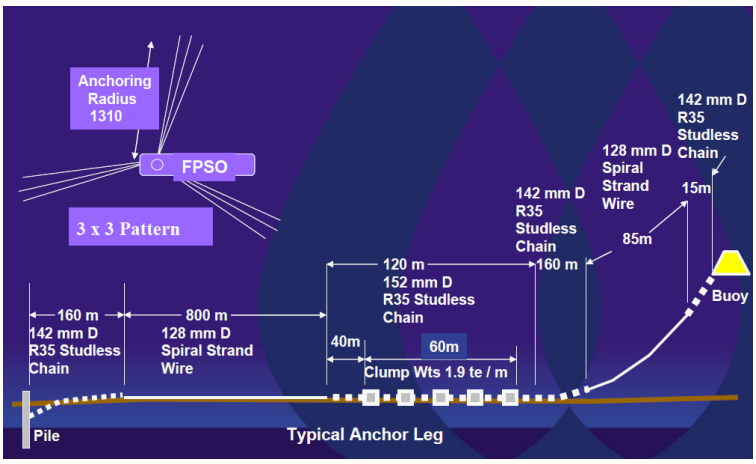

Figure 2.5. Mooring lines arrangement at White Rose (Clark, 2008)

As stated in Norman et al. (2008), to the date of the article (3 years of operation) there have been no disconnections resulting from ice or other environmental events. As well as Terra Nova FPSO, SeaRose is being successfully used for oil production in harsh weather and ice environment, showing promising potential for FPSO use in the sub-Arctic and Arctic regions.

2.3. Prospective FPSO operation at Shtokman field

One of the nearest-future field development with use of a floating production unit is planned to be of the Shtokman gas condensate field. Shtokman field is located approximately 600 km northeast of Murmansk in the Russian sector of the Barents Sea. The water depth at location is about 340 metres (Potapov et al., 2001).

The Shtokman field area is characterized by severe environment, including:

- Extreme waves, winds and current;
- Polar lows;
- Extremely low water and air temperatures;
- Continuous darkness;
- Sea ice, ice ridges and icebergs;
- Icing;

Such harsh environmental conditions in combination with big distances to shore make the development of the Shtokman field one of the most challenging in the world.

The complexity of the field development is to a large extent connected with ice-related challenges. The ice conditions in the area are represented by sea ice, large ice ridges and icebergs. Despite a big hazard of ice actions, the presence of ice (sea ice, ice ridges or icebergs) at location is relatively rare event. Sea ice does not form at Shtokman but is exposed from the North-Northeast by persistent winds, and it occurs at the location approximately once every 2.6 years (Edmond et al., 2011). Sea ice is represented by first-year ice but its thickness can reach up to 2 metres at 100-year condition. Another critical ice-related concern is the presence of ice ridges which imposes big hazard when interacting with a structure. The keel depth of an ice ridge can be up to 21 metres (100-year condition).

The invasion of icebergs is expected to be rare. Observations show that icebergs have been detected near Shtokman (within 75 nautical miles) only about once every five years on average (Edmond et al., 2011). The probability of iceberg impact on the floating production unit is estimated to be less than once within the life duration of the project (50 years) (Marechal et al., 2011). However, despite low probability of accident, the presence of icebergs drives design criteria for the FPSO taking into account possible iceberg impact.

Basing on environmental conditions described above, several FPU designs were proposed for the Shtokman field development. Potapov et al. (2001) describe conceptual design of floating production system for Shtokman proposed by CDB "Coral" and Krylov Shipbuilding Research Institute. The proposed FPSO design includes the following main technical features (note that a lot of them were the state of the art that time):

- Quick disconnect system;
- Ice-strengthened hull (double side and double bottom);
- Retractable rotatable thrusters assisting FPSO vaning;
- Azipod thrusters capable of breaking ice formations;
- Turret mooring system.

An interesting attribute of the design proposed is FPSO equipment by eight 800 kW (each) water jets intended to break ice fields and make an ice lane around the vessel. The FPSO design was tested in an ice tank and proved the feasibility of the Shtokman development concept using moored floating production vessels.

The concept of circular FPSO was also considered for the Shtokman field development (Sevan Marine, 2010, Srinivasan et al., 2011). Having the same ice driven design components, it provides several significant benefits compared to conventional ship-shaped FPSO. As the hull has equal performance in all directions, the weather vaning is no more needed. It also provides an independence of load conditions on the ice drift direction which can change frequently and very fast. Another significant advantage of a circular FPSO is that an ice sheet fails in bending and ice crushing along vertical sides does not occur. The principal layout of a circular FPSO is presented in Figure 2.6.

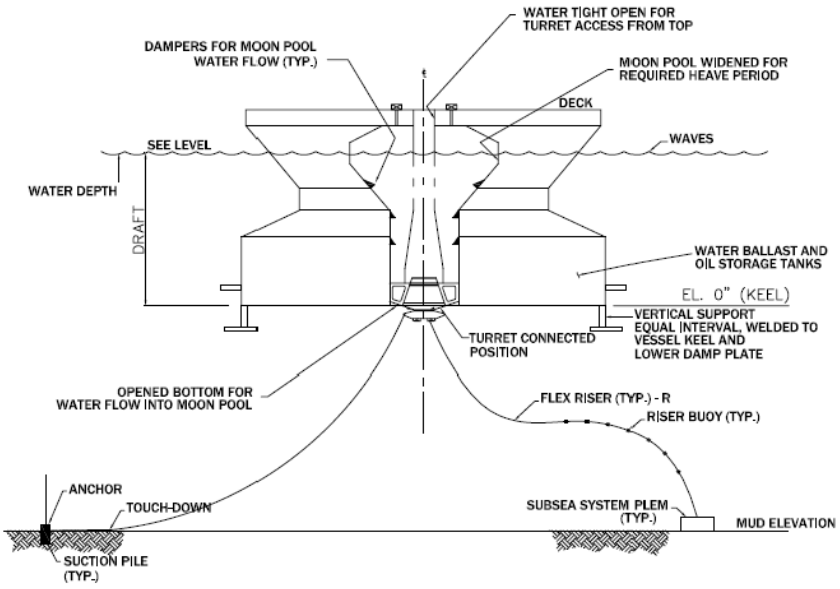

Figure 2.6. Principal layout of a circular FPSO (Srinivasan 2011)

Despite several FPU designs proposed for the field, Shtokman Development AG (an operator of the first phase of the field development) has concluded to design the floating platform as a turret moored disconnectable and ice-resistant ship shaped floating platform (Le Marechal et al., 2011). Le Marechal et al (2011) besides the harsh Arctic environmental condition emphasize another challenge of the project connected with the fact that it is the first development in the region. It means that logistic base and infrastructure will have to be developed. Le Marechal et al. (2011) proposed some specific principles of floating production unit design for Shtokman conditions. The concept of FPU proposed is designed to withstand almost all ice and iceberg actions occurred at Shtokman. The main ice-related design limits of the design proposed are (Le Marechal et al., 2011):

- The mooring system has to withstand vessel's head-on interaction with 100-year ice ridge at Ultimate Limit State (ULS) with corresponding safety factor;
- The mooring system has to be able to withstand ship's ice-vaning in unmanaged 100-year level ice at ULS with corresponding safety factor;
- The mooring system has to withstand during vessel's head-on interaction with 10,000-year iceberg in open water at ULS with corresponding safety factor;
- The mooring system has to withstand 5,000 tonnes horizontal load at ULS;
- Disconnection system has to be able to operate under a mooring load at least 2,500 tonnes at ULS with corresponding safety factor;
- Hull has to be reinforced to resist all sea ice conditions and interaction scenarios corresponding to the maximum mooring capacity. In other words, mooring is damaged first, while hull is safe;
- Emergency disconnection has to be performed in 3 minutes;

- The vessel's offset capacity for the risers has to be larger than that for the mooring.
- Direct contact between mooring lines and icebergs has to be avoided. Under hull ice transport has to be minimized (avoided).

The FPSO's hull has been designed to satisfy design limits and to enhance its performance in ice. One of the features is that the bow is designed with high icebreaking capabilities, allowing breaking level ice and ice ridges. The bow is also specifically designed to take loads due to iceberg interaction in the most efficient way. The hull sides are ice-strengthened to resist ice loads during ice-vaning and due to interactions with level ice, broken ice, ice ridges or icebergs. Another attribute of the hull design is inclined sides, enabling ice failure in bending in an ice-vaning situation. The FPSO design proposed was comprehensively tested in ice tanks and proved its excellent performance in ice.

CHAPTER 3: OVERVIEW OF NUMERICAL SIMULATIONS OF ICE-STRUCTURE INTERACTION

This section presents several examples of numerical models with the purpose to introduce a reader to general ideas of simulation of ice-structure interaction. Since the present work deals with FPSO (i.e. moored ship) behaviour in level ice, this section mainly focuses on the simulations of ice-ship interaction and ice sheet-structure interaction.

3.1. Simulation of ice field behaviour and interaction with a structure

Finite Element Method (FEM)

Gürtner (2009) has investigated both experimentally and numerically the ice-structure interaction. His work is devoted to investigation of the ice barrier concepts – Ice Protection Piles (IIP) and Shoulder Ice Barrier (SIB). The numerical model of Gürtner (2009) is based on the finite element method focusing on comprehensive investigation of dynamic fracture propagation. The dynamic fracture propagation is simulated by so-called Cohesive Zone Model (CZM), which allows satisfaction of conservative laws. The main idea of the CZM is the placing interface elements with certain mechanical properties between two neighboring finite elements. Such representation allows simulation of crack propagation taking the fracture process zone into account and without violation of conservative laws. The method used in the model of Gürtner (2009) is called Computational Cohesive Element Model (CCEM), which implies implementation of CZM into a multi-material model. The numerical model proposed by Gürtner (2009) was applied to simulate the interaction of an ice sheet with ice protection piles. The simulation was intended to investigate the influence of piles arrangement on interaction with ice. The results obtained by the numerical model well agreed with the results of the model tests. The CCEM was also used to investigate ice interaction with Shoulder Ice Barrier. The numerical results showed fairly good agreement with the experimental investigations.

Blackerby (2006) investigated ice sheet actions on conical structures for Bohai Bay, China, by means of finite element method. ANSYS and LS-DYNA commercial program packages were employed in his work. In this simulation the cracks in ice sheet were not modeled but were just assumed to occur at the places where the stress values overcome the yield stress of ice. The subjects of investigation were: (1) the influence of the contact width between an ice sheet and a structure on the interaction, (2) the influence of approaching velocity on stress distribution in the ice sheet and (3) the influence of cone angle on the interaction process.

Discrete Element Method (DEM)

Løset (1994a) has developed a two-dimensional numerical model for simulation of a broken ice field dynamics based on discrete element method. The broken ice field in this model is represented by circular disks of different diameters and brash ice between them. The model applies "soft" particles approach which implies that the overlapping of the ice floes is allowed. The contact forces of direct interaction between floes are assumed to have visco-elastic-plastic behaviour represented by a set of elastic springs, dashpots and friction elements. Therefore, the interaction forces are dependent on the area of overlap and the relative velocity. The contact forces can also occur "remotely" by squeezing brash ice between the floes. An effective method

of finding the disks in contact based on a cell structure of a domain was applied allowing significant reduction of calculation time. The model was employed to simulate ice forces exerted on a boom when it is pulled through a broken ice field (Løset, 1994b). The model was calibrated by comparison with the experimental results obtained in an ice tank.

Hopkins (1992) applied Discrete Element Model (DEM) for simulation of ice ridging process. The author represented an ice sheet by a set of glued discrete convex polygons. The edges of neighboring polygon blocks are assumed to be joined by viscous-elastic fibers. Due to deformations in the ice sheet, the polygons move relative to one another and the imaginary fibers stretch or compress, creating inter-particle forces. The failure of an ice sheet occurs when the stress in the fiber at either end of the joint exceeds the compressive or tensile strength of the material. In that case the crack between two adjacent polygons is assumed to propagate at a constant specified velocity. Along the cracked part of a joint the tensile stress is no more exerted. Hopkins (1992) has applied the glued joint approach to simulate floating beam on an elastic foundation and compared with analytical solution. The good agreement has proven the feasibility of the approach. Then the glued joint approach was used to simulate sea ice ridging.

Hopkins and Tukhuri (1999) have proposed an approach to simulate ice jam formation, pressure ridges formation and the dynamics of broken ice fields. The approach proposed is based on three-dimensional DEM. The broken ice field in the model is represented by dilated circular disks with circular edges (see Hopkins, 2003). The approach was applied to simulate the compression of ice field represented by circular ice disks by a pusher. As the authors state, this problem can be important for e.g. clearance of the sea from the ice floes in the case of oil spill. The simulation also assists understanding of ice jam and ridges formation. The feasibility of the numerical model was validated by compliance with the results of model test carried out by Hopkins and Tukhuri (1999).

Jirásek and Bažant (1995) proposed a two-dimensional numerical model based on discrete element method to investigate fracture of brittle materials with regard to an ice sheet - structure interaction. The ice sheet is represented by an ensemble of particles interconnected by elastic links with the neighboring ones. The interaction between the particles is assumed to be only in normal direction. The key attribute of the model consists in the microlevel constitutive law for each inter-particle link, which may be represented as bilinear. That is, the stress firstly growth with increasing the strain, but after reaching a peak starts to decrease with the strain increase. When stress in a link reaches the tensile strength of the material, the link is eroded. Such representation allows description of progressive distributed microcracking with gradual softening and with a large cracking zone. As the regular lattice arrangement showed directional bias, the random particle distribution was proposed by the authors.

Particle-In-Cell (PIC) method

Barker et al. (2000a) applied particle-in-cell (PIC) concept for simulation of pack ice field behaviour. The PIC method represents the problem formulation with mixed Lagrangian and Eulerian points of view. The total ice volume of the domain considered is partitioned into a number of individual particles. Each particle has a constant volume which is characterized by its thickness and area. The motion of particles is treated in Lagrangian manner, i.e. in the particle-fixed coordinate system. The particles do not represent actual ice floes but they are used as

computational elements. The domain under consideration is partitioned into Eulerian (fixed) grid.

In the Eulerian grid for each cell the ice thickness and concentration are determined from the information on particles presented in the cell. Then for each node of fixed grid the velocities are calculated, which are further interpolated to the particle locations by means of interpolation functions (conversion to the Lagrangian coordinate system). The new positions of particles are determined. Identifying particles in cell, the values of ice concentration and ice thickness are updated for the cell. Due to constant volume of particles, in the case when concentration exceeds the unity, the ice thickness of the particle is assumed to increase. Such a way, the particle-in-cell concept allows description of rubble accumulation that makes this method very efficient for simulation of ice-structure interaction.

Barker et al. (2000a) used this concept to simulate pack ice loads on a bridge pier in the White River, Vermont. The peak load predicted by the model was in very good agreement with the data obtained by full-scale study. However, time-series loads differed significantly for the two cases (Barker et al., 2000a). The PIC method was also applied for simulation of ice loads on the "Kulluk" drilling vessel (Barker et al., 2000b). A fairly good compliance of predicted loads with full-scale measurements was obtained.

3.2. Simulation of ice-ship interaction

Hansen and Løset (1999a) investigated behaviour of floating offshore units moored in broken ice. For this purpose a two-dimensional numerical model based on discrete element method was developed. Behaviour of a broken ice field is described on the ground of the numerical model created by Løset (1994), the overview of which is presented above. In order to verify the numerical model, the results were compared with data obtained by the model test of a Submerged Turret Loading in ice carried out in an ice tank (Hansen and Løset, 1999b). The comparison revealed good qualitative compliance. A good quantitative agreement of the results was also reached, however, some minor discrepancies occurred. These discrepancies in the results are explained by different setups for the numerical and experimental tests. Nevertheless, the numerical model proved feasible to simulate moored vessel behaviour in broken ice.

Aksnes and Bonnemaire (2009) proposed a simplified approach for modelling stochastic response of moored vessels in level ice (Aksnes, 2011). Only a single-degree-of-freedom vessel's motion in level ice, namely surge, was under consideration. In the model proposed an ice sheet is treated as an elastic beam consisting of parts with stochastic properties. The randomness is introduced by setting the ice thickness, ice breaking length, temperature and salinity for each part from the prescribed distribution. The governing mechanical parameters, namely the modulus of elasticity E and flexural strength σ_f, are then calculated by the known formulae from temperature and salinity. The results of the time-domain simulation have revealed non-linear effects in behaviour of a moored vessel for very low ice drift speed.

Su et al. (2009) elaborated upon ship performance in level ice. A two-dimensional numerical model with three degrees-of-freedom motion of a vessel has been developed. The attribute of the numerical model consists in simulation of continuous ice breaking process, contrary to the common approach based on break-displace process. Wedged edges of an ice sheet and ship's hull are represented by an ensemble of nodes, enabling determination of non-

simultaneous contact. The numerical model implies employment of parameters estimated by empirical coefficients, such as ice failure load, icebreaking radius and compressive strength. The numerical model has been validated by comparison with full-scale data of performance in level ice obtained for the Tor Viking II icebreaker in terms of *h*-*v* relation. The comparison in terms of turning circle diameter has also shown good agreement.

CHAPTER 4: NUMERICAL SIMULATION OF AN ICE SHEET BENDING

4.1. Description of the numerical model of an ice sheet bending

The numerical model of an ice sheet bending has been developed in the thesis. The model is based on the plate theory. The numerical model has been developed with the main purpose of grounding the evaluation of ice failure load, which essentially influences the horizontal loads exerted to a vessel interacting with level ice.

The plate is known to be a prismatic body limited by two parallel planes, the distance between which is much less than other characteristic dimensions (Sachenkov, 2012). Three types of plates have to be distinguished: (1) thin plate with small deflections, (2) thin plates with large deflections and (3) thick plates (Timoshenko and Woinowsky-Krieger, 1989). The first two types of plates allow simplification of the problem to two-dimensional problem of elasticity, while the theory of thick plates requires solution of three-dimensional problem. In the theory of thin plates all stress components can be expressed by deflection *w*, which is a function of two coordinates in the plane of the plate. Thus, the solution of thin plate problem can be significantly simplified, practically without loss of accuracy.

Ice sheet is ideally fit for the definition of thin plate, and therefore the theory can efficiently be applied for consideration of ice sheet-structure interaction.

Governing equations

The developed numerical model is capable of calculating all types of thin plate bending. The mathematical foundation for calculation of these problems is briefly described below.

Thin plate with small deflection

If deflection *w* of a plate is small in comparison with its thickness *h*, the solution of the problem can be significantly simplified by applying the following assumptions (Timoshenko and Woinowsky-Krieger, 1989):

- There is no deformation in the middle plane of the plate. This plane remains neutral during bending;
- Points of the plate lying initially on a normal-to-the-middle plane of a plate remain on the normal-to-the-middle surface of the plate after bending;
- The normal stresses in the direction transverse to the plate can be disregarded.

Based on these assumptions, the solution of the problem is reduced to the solution of biharmonic equation for deflection with associated boundary conditions:

$$\frac{\partial^4 w}{\partial x^4} + 2\frac{\partial^4 w}{\partial x^2 \partial y^2} + \frac{\partial^4 w}{\partial y^4} = \frac{q}{D} \tag{4.1}$$

or in the symbolic form:

$$\Delta\Delta w = \frac{q}{D}$$

where w is plate deflection;

q is a lateral load;

D is flexural rigidity of a plate;

$$\Delta w = \frac{\partial^2 w}{\partial x^2} + \frac{\partial^2 w}{\partial y^2}$$

According to the first assumption, the theory of thin plates with small deflection implies the absence of stresses in the middle plane. However, this assumption is not fully valid for the problem of ice sheet - structure interaction, since significant loads can occur in the middle plane of the ice plate. Therefore, the problem of thin plate with small deflection under combined lateral load and forces in the middle plane is worth being considered.

Thin plate with small deflection under combined lateral load and forces in the middle plane

Sachenkov (2012) has clearly shown that when deflection of plate is small, the problem of the plate bending under combined action of lateral load and forces in the middle plane can be divided into two separate problems: (1) the problem of thin plate bending with small deflection and (2) the plane problem of elasticity (plane stress or plane strain).

According to Wang (1996), if the dimension normal to the plane of interest is much less than the in-plane dimensions, then such problem is stated as plane stress problem. Since the ice thickness is much less than other characteristic dimensions of an ice sheet, the plane stress problem has to be considered. Sedov (1994) states that the plane problem in the theory of elasticity can be solved by integrating the biharmonic equation for Airy function with associated boundary and single-valuedness conditions:

$$\frac{\partial^4 U}{\partial x^4} + 2\frac{\partial^4 U}{\partial x^2 \partial y^2} + \frac{\partial^4 U}{\partial y^4} = 0 \tag{4.2}$$

where U is the Airy function which is defined as:

$$\sigma_{xx} = \frac{\partial^2 U}{\partial y^2}; \tag{4.3}$$

$$\sigma_{yy} = \frac{\partial^2 U}{\partial x^2}; \tag{4.4}$$

$$\sigma_{xy} = -\frac{\partial^2 U}{\partial x \partial y} \tag{4.5}$$

Thus, the problem of plate bending with small deflection undergone a combined action of lateral load and forces in the middle plane is reduced to the separate solutions of two biharmonic equations with corresponding boundary conditions:

$$\begin{cases} \Delta\Delta w = \frac{q}{D} \\ \Delta\Delta U = 0 \end{cases} \tag{4.6}$$

where $\Delta = \frac{\partial^2}{\partial x^2} + \frac{\partial^2}{\partial y^2}$

However, specification of boundary conditions for Airy function represents some challenges. It is connected with the fact that usually plane stress problem is stated with boundary conditions established either in terms of stresses or displacements. Specification of boundary

conditions for Airy function in terms of stresses gives a number of constants after integration of the equations (4.3)-(4.5). Determination of these constants represents specific problem.

The plane stress problem can be alternatively solved in terms of displacements. In that case the governing equations are given as:

$$\begin{cases} \dfrac{\partial^2 u}{\partial x^2} + \dfrac{1}{2}(1+\nu)\dfrac{\partial^2 v}{\partial x \partial y} + \dfrac{1}{2}(1-\nu)\dfrac{\partial^2 u}{\partial y^2} = 0 \\ \dfrac{\partial^2 v}{\partial y^2} + \dfrac{1}{2}(1+\nu)\dfrac{\partial^2 u}{\partial x \partial y} + \dfrac{1}{2}(1-\nu)\dfrac{\partial^2 v}{\partial x^2} = 0 \end{cases} \tag{4.7}$$

In such formulation, it is important to make sure that the displacement components satisfy the Saint-Venant's equations for strain continuity.

Thus, such formulation of the plate bending problem allows determination of stresses in the middle plane. This is essential in consideration of ice sheet failure. However, in such formulation of problem the stresses in the middle plane do not have influence on the bent state of the plate. This means that stresses in the middle plane do not affect bearing capacity of an ice sheet. This is valid only for small deflection of a plate.

The deflection of an ice sheet before failure is known to be small. Therefore, there expected to be only minor contribution to the bearing capacity of an ice sheet due to stresses in the middle plane. However, in order to prove it, the problem of bending of thin plates with large deflection is also solved in the present numerical model.

Thin plate with large deflection

Lack of deformation in the middle plane is completely valid only when a plate is bent into a developable surface, i.e. the dimensions of the middle plane remain unchanged. (For example, when a plate is bent to the cylindrical surface and its edges are free to move). In other cases, plate bending is accompanied with strain in the middle plane. This strain may have significant contribution to the bearing capacity of a plate when deflection is not small.

The governing system of equations for this kind of problem is given as:

$$\begin{cases} \left(\dfrac{\partial^4 w}{\partial x^4} + 2\dfrac{\partial^4 w}{\partial x^2 \partial y^2} + \dfrac{\partial^4 w}{\partial y^4}\right) = \dfrac{1}{D}\left(q + N_x \cdot \dfrac{\partial^2 w}{\partial x^2} + N_y \cdot \dfrac{\partial^2 w}{\partial y^2} + 2N_{xy}\dfrac{\partial^2 w}{\partial x \partial y}\right) \\ \dfrac{1}{Eh}\left(\dfrac{\partial^2 N_x}{\partial y^2} + \dfrac{\partial^2 N_y}{\partial x^2} - 2\dfrac{\partial^2 N_{xy}}{\partial x \partial y}\right) = \left(\dfrac{\partial^2 w}{\partial x \partial y}\right)^2 - \dfrac{\partial^2 w}{\partial^2 x}\dfrac{\partial^2 w}{\partial^2 y} \\ \dfrac{\partial N_x}{\partial x} + \dfrac{\partial N_{xy}}{\partial y} = 0 \\ \dfrac{\partial N_y}{\partial y} + \dfrac{\partial N_{xy}}{\partial x} = 0 \end{cases} \tag{4.8}$$

where N_x, N_y and N_{xy} are forces per unit length in the middle plane;

E is modulus of elasticity;

h is ice thickness.

Non-linearity of the system of equations presented above significantly complicates its solution.

Calculation of main mechanical parameters

Displacement in the middle plane

Thin plate with small deflection

$u_0 = 0$
$v_0 = 0$

Thin plate with small deflection under combined lateral load and forces in the middle plane

Displacement components u_0 and v_0 in this problem are found by solving linear system of equations (4.7) with prescribed boundary conditions.

Thin plate with large deflection

Displacement components u_0 and v_0 in this problem are found by iteratively solving the equations of the system (4.8). In the first iteration the displacement components u_0 and $v_0$and forces in the middle plane are set equal to zero.

1) With values of forces in the middle plane obtained in the previous iteration, the deflection *w* is found by solving the first equation of the system (4.8).
2) With the values for deflection obtained, the last two equations of the system (4.8) are solved in terms of displacement components u_0 and v_0. (The second equation of the system (4.8) indeed represents the Saint-Venant's equation expressed in terms of forces in the middle plane).
3) Then the forces in the middle plane are found as:

$$N_x = \frac{Eh}{1-\nu^2}\left[\frac{\partial u_0}{\partial x} + \frac{1}{2}\left(\frac{\partial w}{\partial x}\right)^2 + \nu\frac{\partial v_0}{\partial y} + \frac{\nu}{2}\left(\frac{\partial w}{\partial y}\right)^2\right] \tag{4.9}$$

$$N_y = \frac{Eh}{1-\nu^2}\left[\frac{\partial v_0}{\partial y} + \frac{1}{2}\left(\frac{\partial w}{\partial y}\right)^2 + \nu\frac{\partial u_0}{\partial x} + \frac{\nu}{2}\left(\frac{\partial w}{\partial x}\right)^2\right] \tag{4.10}$$

$$N_{xy} = \frac{Eh}{2(1+\nu)}\left[\frac{\partial u_0}{\partial y} + \frac{\partial v_0}{\partial x} + \frac{\partial w}{\partial x}\frac{\partial w}{\partial y}\right] \tag{4.11}$$

4) The procedure of items 1 through 3 is repeated until the required accuracy is obtained.

Hereafter we will consider only the problem of thin plate with large deflection as the most general case, since it is obvious that the other two problems can be easily obtained by setting the number of iterations equal to one. Note that for the problems with small deflection the non-linear terms will be canceled.

Displacement components

$$u = -\frac{\partial w}{\partial x} z + u_0 \tag{4.12}$$

$$v = -\frac{\partial w}{\partial y} z + v_0 \tag{4.13}$$

Stresses in the plate

$$\sigma_x = -\frac{Ez}{1-\nu^2}\left(\frac{\partial^2 w}{\partial x^2} + \nu \frac{\partial^2 w}{\partial y^2}\right) + \sigma_{x0}$$

$$\sigma_y = -\frac{Ez}{1-\nu^2}\left(\frac{\partial^2 w}{\partial y^2} + \nu \frac{\partial^2 w}{\partial x^2}\right) + \sigma_{y0}$$

$$\sigma_z = 0$$

$$\tau_{xy} = -\frac{Ez}{1+\nu}\frac{\partial^2 w}{\partial x \partial y} + \tau_{xy0}$$

$$\tau_{xz} = \frac{E(z^2 - \frac{h^2}{4})}{2(1-\nu^2)}\frac{\partial}{\partial x}\Delta w - \frac{E(z - \frac{h}{2})}{1-\nu^2} \cdot \left[\frac{\partial^2 u_0}{\partial x^2} + \frac{1+\nu}{2}\frac{\partial^2 v_0}{\partial x \partial y} + \frac{1-\nu}{2}\frac{\partial^2 u_0}{\partial y^2} + \frac{\partial w}{\partial x}\frac{\partial^2 w}{\partial x^2} + \frac{1+\nu}{2}\frac{\partial w}{\partial y}\frac{\partial^2 w}{\partial x \partial y} + \frac{1-\nu}{2}\frac{\partial w}{\partial x}\frac{\partial^2 w}{\partial y^2}\right] \tag{4.14-4.18}$$

$$\tau_{yz} = \frac{E(z^2 - \frac{h^2}{4})}{2(1-\nu^2)}\frac{\partial}{\partial y}\Delta w - \frac{E(z - \frac{h}{2})}{1-\nu^2} \cdot \left[\frac{\partial^2 v_0}{\partial y^2} + \frac{1+\nu}{2}\frac{\partial^2 u_0}{\partial x \partial y} + \frac{1-\nu}{2}\frac{\partial^2 v_0}{\partial x^2} + \frac{\partial w}{\partial y}\frac{\partial^2 w}{\partial y^2} + \frac{1+\nu}{2}\frac{\partial w}{\partial x}\frac{\partial^2 w}{\partial x \partial y} + \frac{1-\nu}{2}\frac{\partial w}{\partial y}\frac{\partial^2 w}{\partial x^2}\right]$$

(the latter two equations are found from the static equilibrium, but they do not represent big interest, since they are not used for further calculations)

where z is the vertical coordinate;

σ_{x0}, σ_{y0}, τ_{xy0} are stress components in the middle plane, which are given as:

$$\sigma_{x0} = \frac{E}{1-\nu^2} \cdot \left[\frac{\partial u_0}{\partial x} + \frac{1}{2}\left(\frac{\partial w}{\partial x}\right)^2 + \nu \frac{\partial v_0}{\partial y} + \frac{\nu}{2}\left(\frac{\partial w}{\partial y}\right)^2\right]$$

$$\sigma_{y0} = \frac{E}{1-\nu^2} \cdot \left[\frac{\partial v_0}{\partial y} + \frac{1}{2}\left(\frac{\partial w}{\partial y}\right)^2 + \nu \frac{\partial u_0}{\partial x} + \frac{\nu}{2}\left(\frac{\partial w}{\partial x}\right)^2\right] \tag{4.19-4.22}$$

$$\tau_{xy0} = \frac{E}{2(1+\nu)} \cdot \left[\frac{\partial u_0}{\partial y} + \frac{\partial v_0}{\partial x} + \frac{\partial w}{\partial x}\frac{\partial w}{\partial y}\right]$$

Moments

$$M_x = -D \cdot \left(\frac{\partial^2 w}{\partial x^2} + \nu \frac{\partial^2 w}{\partial y^2}\right) \tag{4.23-4.25}$$

$$M_y = -D \cdot \left(\frac{\partial^2 w}{\partial y^2} + \nu \frac{\partial^2 w}{\partial x^2}\right)$$

$$M_{xy} = -D \cdot (1 - \nu) \frac{\partial^2 w}{\partial x \partial y}$$

Von Mises stress (Sedov, 1994)

$$\sigma_{VM} = \sqrt{\frac{1}{2}\left[\left(\sigma_x - \sigma_y\right)^2 + \left(\sigma_y - \sigma_z\right)^2 + (\sigma_z - \sigma_x)^2 + 6 \cdot \left(\tau_{xy}^2 + \tau_{xz}^2 + \tau_{yz}^2\right)\right]} \quad (4.26)$$

Thus, at the surfaces of the plate the Von Mises stress becomes:

$$\sigma_{VM} = \sqrt{\sigma_x^2 - \sigma_x \sigma_y + \sigma_y^2 + 3\tau_{xy}^2} \quad (4.27)$$

Failure criteria

The failure of an ice sheet is known to be very complicated process. It is connected with complex fracture propagation process in an ice sheet. A comprehensive modelling of ice sheet fracturing by means of Computational Cohesive Element Method (CCEM) has been performed by Gürtner (2009), who investigated ice-structure interaction. Two-dimensional cracking of an ice sheet was simulated by Jirásek and Bažant (1995) based on discrete element method (DEM). However, it is common to apply some simplifications for failure criteria. Thus, for instance, Blackerby (2006) assumed that a circumferential crack occurs if the stress in circumferential direction exceeds the yield stress, while a radial fracture arises in the case if yield stress is exceeded in the radial direction. No further consideration of failure process was applied. For bending of elastic beam it has become conventional to identify failure by flexural strength, though flexural strength is not true material property (Timco, 1984). This approach has then been extended to other types of ice sheet representation. Thus, for instance, Sawamura et al. (2010) in 3D finite element model assumed that bending failure occurs when the surface stress of the ice exceeds the flexural strength of the ice. For our model we follow the same bending failure criteria, however, instead of normal stress at a surface of a plate the Von Mises stress criteria is used. So, as a criteria of an ice sheet failure, we assume that first fracture initiates when the Von Mises stress at one of the surfaces exceeds flexural strength of ice.

4.2. Capabilities and limitations of the numerical model developed

Capabilities

The numerical model was developed with the purpose to introduce a mathematical tool to evaluate ice failure load and to assist understanding of different failure mechanisms. The numerical model developed in this thesis allows:

- *Calculation of deflection of an ice sheet under specified lateral loads*
  The lateral loads can be exerted at any point of a domain. This capability of the model developed is very useful in consideration of interaction between an ice sheet and a sloping or conical structure. This kind of problem is relevant when ice sheet is interacting with a sloping or conical structure having relatively gentle slope and ice rubble

accumulation at the structure does not create significant resistance to the ice sheet advancement. Another possible problem that can be solved by means of the model developed is a bearing capacity of the ice sheet.

- *Determination of lateral loads from prescribed deflection (inverse problem)*
  The deflection can be predetermined at any point of a domain. The model developed permits calculation of the lateral loads needed to set an ice sheet into the prescribed bent state. As an example of application of this feature, the model can be used to determine loads on a structure when position of an ice sheet is known. Using this capability of the model and knowing the velocity of the ice sheet advancement, the loads exerted to the structure can be calculated in time domain. So, despite the model is static, the problem of ice sheet - structure interaction can be indirectly solved in time domain.

- *Solution of plane stress problem*
  This capability of the numerical model developed can be applied for examination of ice sheet interaction with a vertical structure. The external forces acting in the plane of the sheet or displacements can be prescribed at any point of the domain's boundary. The model allows calculation of parameters such as stresses, strains, displacements and Von Mises yield criteria.

- *Calculation of deflection of an ice sheet under predetermined combined lateral and in-plane loads*
  This feature becomes very important when there are considerable forces acting in the middle plane, since they change the bent state of a sheet and can significantly change ice failure mode. This problem becomes of profound interest when ice rubble accumulates at a structure. Another situation when the consideration of this problem is essential is interaction of an ice sheet with a steep slope, since besides bending local crushing occurs.

- *Calculation of essential parameters*
  In each mode presented above the model developed allows calculation of the principal parameters such as plate deflection, associated bending and shearing moments, stresses and strains, displacements and Von Mises yield criteria in every point of the domain.

- *Prediction of failure mode*
  By identifying the areas where the failure criteria is reached (namely, Von Mises stress is higher than yield strength of ice) the model assists in prediction the type of a failure mode – crushing , semi-infinite elastic beam failure mode, plate failure mode or wedged beam failure mode.

Limitations

- The ice sheet is treated as homogeneous, purely elastic plate.
- The numerical model of ice sheet bending is static. However, dynamic problems can be solved by method of sequential changing of static states.
- Due to static nature of the numerical model velocity effects are not taken into account.

- Due to computational limitations, mesh size of the grid applied for FDM is limited by the certain minimum value.
- In the present work only rectangular ice sheet domain was modeled.
- So far the numerical model does not simulate fracture propagation. Therefore, the failure pattern is not able to be determined.

4.3. Modeling of different failure modes

Determination of ice breaking length represents quite a challenging task, since field observations show that this parameter may vary in a wide range (Li et al., 2003). Li et al. (2003) performed full-scale tests on the offshore platform JZ20-2 in the Bohai Bay with the purpose to establish dependence between the ice breaking length and main influencing parameters. The platform is a 4-leg jacket with cones installed on each leg in order to reduce vibrations on the structure. The deflecting device installed on each leg includes an upward cone with angle of 60 degrees and a downward cone with 30 degrees angle. The cross-section connecting these two cones has a diameter of 4.6 metres.

In order to examine the dependence of breaking length on influencing parameters, Li et al. (2003) proposed to use two non-dimensional variables, namely breaking length/ice thickness ratio l_b/h and the structure diameter/ice thickness ratio D/h.

Lau et al. (1999), cited by Li et al. (2003), classify the bending failure process into three modes:

- Semi-infinite beam mode;
- Plate failure mode;
- Wedged beam failure mode;

Semi-infinite beam mode dominates when the loading is evenly distributed along whole front boundary of an ice sheet, or at least the width of the boundary loaded significantly exceeds the ice thickness (Li et al. 2003). In this case the ice sheet can be regarded as a beam on an elastic foundation. The semi-infinite beam mode produces very large breaking length.

According to Li et al. (2003), *plate failure mode* occurs when the load is also distributed along the front boundary of an ice sheet, but the boundary is not very wide. Therefore, lateral deformation of the ice sheet contributes to the picture. In the plate failure mode, circumferential crack initiates first and then is followed by the radial crack propagation. The breaking length in this failure mode is the least among others.

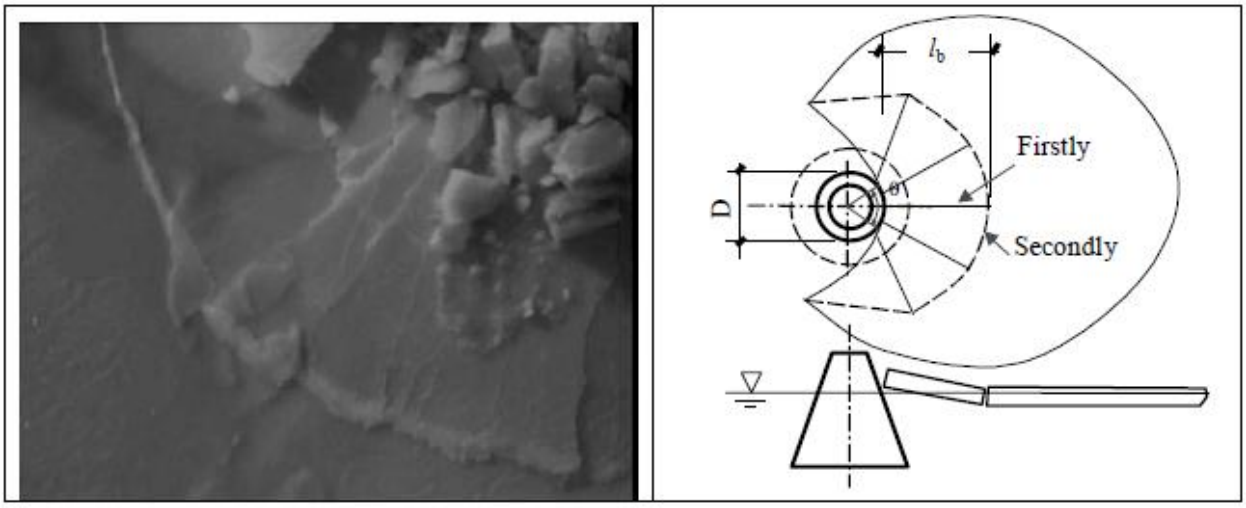

Figure 4.1: Wedge beam failure mode observed in Bohai Bay (Li et al., 2003)

Wedge beam failure mode occurs when the loading boundary is a narrow line in the order of ice thickness (Li et al., 2003). The ice sheet undergoes bending in both lateral directions. Due to the narrow loading line, the maximum curvature of the ice sheet, and consequently the maximum bending moment, occurs at the contact with a structure. Therefore, the failure initiates near the structure and then propagates radially. Subsequently, circumferential cracks connect radial failure, breaking ice into wedged blocks. This type of bending failure mode is characterized by medium breaking length.

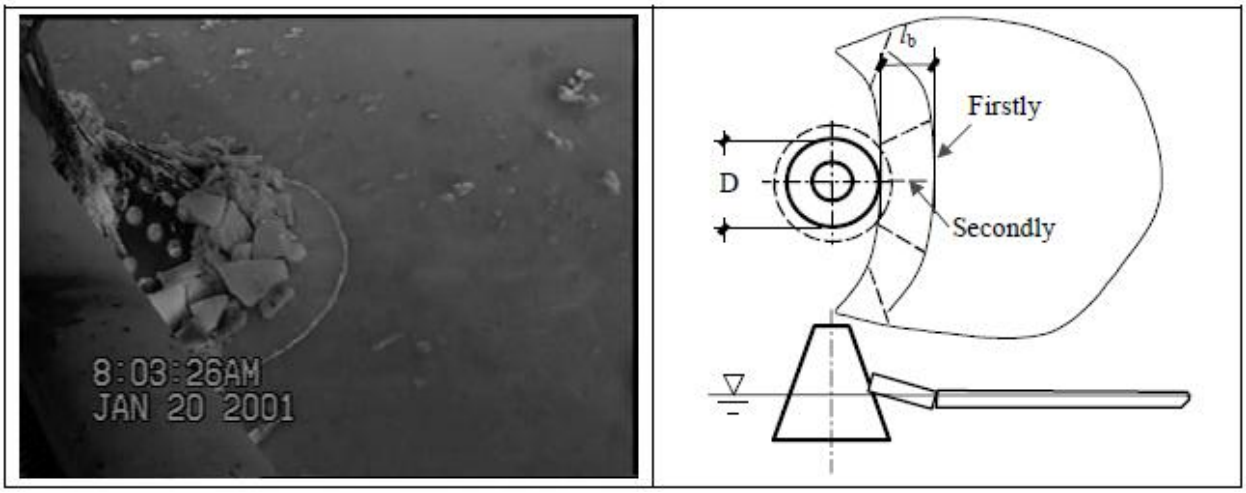

Figure 4.2: Plate failure mode observed in Bohai Bay (Li et al., 2003)

Li et al. (2003) state that during field observations of ice sheet - conical structure interaction in Bohai Bay no failure of semi-infinite beam type was indicated. Two other types of bending failure, namely plate bending and wedge beam bending, occurred separately and in a mixed mode. The results of full-scale test showed that the mean length/thickness ratio was 6.9 and 3.4 for wedged beam bending failure and plate type failure respectively. In transition failure mode between the latter two the mean breaking length/ thickness ratio was about 5 (Li et al., 2003).

The authors elaborated on the reasons that control the failure mode. They concluded that the main influencing parameter determining transition between wedged beam and plate mode is the width of contact. They also identified that the presence of ice rubble also affects the bending failure mode. A reason for that consists in the fact that ice rubble increases the contact width, therefore a transition to the plate bending failure mode is likely to occur. According to Li et al. (2003) mechanical properties of ice, such as elasticity and ductility, also have influence on bending failure mode. Another influencing parameter is ice velocity.

Let us now make an attempt to predict bending failure mode of ice by means of the model developed. It is assumed in the model, basing on the paper of Sawamura et al. (2010), that bending failure occurs when the Von Mises stress at surface of a plate exceeds ice flexural strength. Let us first look into the situations presented as an example in the paper of Li et al. (2003) (see Figure 4.1 and Figure 4.2). The parameters assumed (since we do not know exactly) for these situations are listed in Table 4.1.

Table 4.1: Parameters assumed for simulation

Property	***Situation 1***	***Situation 2***
Modulus of elasticity, E	5.4 GPa	5.4 GPa
Poisson ratio, ν	0.3	0.3
Ice thickness, h	0.1 m	0.1 m
Cone diameter at the ice level, D	2.5 m	4.5 m
Diameter/thickness ratio, D/h	25	45
Flexural strength	0.75 MPa	0.75 MPa

Now using the model developed we simulate two ice states corresponding to the failure limit.

The interaction with a conical structure occurs not simultaneously along the cone, but takes place on the relatively narrow contact area. The real width of the contact area plays essential role in the determination of bending failure pattern. It is quite challenging to determine real contact width, since a number of processes should be taken into account, such as crushing, deformation etc. In order to determine the real width of contact area between an ice sheet and the cone in our model we follow the ideas of Su et al. (2009), who assumed that before bending failure local ice crushing occurs at the contact up until the moment when the vertical force is sufficient to break the ice in bending (see sketch in **Figure 4.4**).

In order to find the width of contact corresponding to the bending failure, we implement so-called "nodal analysis". The idea of this method is to calculate the vertical force necessary to break ice in failure for varying contact width and independently calculate vertical forces corresponding to local crushing for varying contact width. The intersection of these two dependences gives us the actual contact width (the point when "the vertical force we need" is equal to "the vertical force we have").

Using the model developed we calculate the vertical force needed to break an ice sheet in bending. The results obtained for the ice thickness of 0.1 metres are summarized in **Table 4.2** and an example of the model run in terms of Von Mises stress is illustrated in **Figure 4.3.**

Table 4.2: Results of the numerical simulation – failure loads for varying contact width

Contact width (chord)	Vertical force corresponding to failure in bending
0.5 [m]	3.25 [kN] (wedged beam)
1 [m]	4.5 [kN] (wedged beam)
1.5 [m]	4.9 [kN] (wedged beam)
2 [m]	5.5 [kN] (circumferential)
2.5 [m]	5.6 [kN] (circumferential)
3 [m]	5.7 [kN] (circumferential)

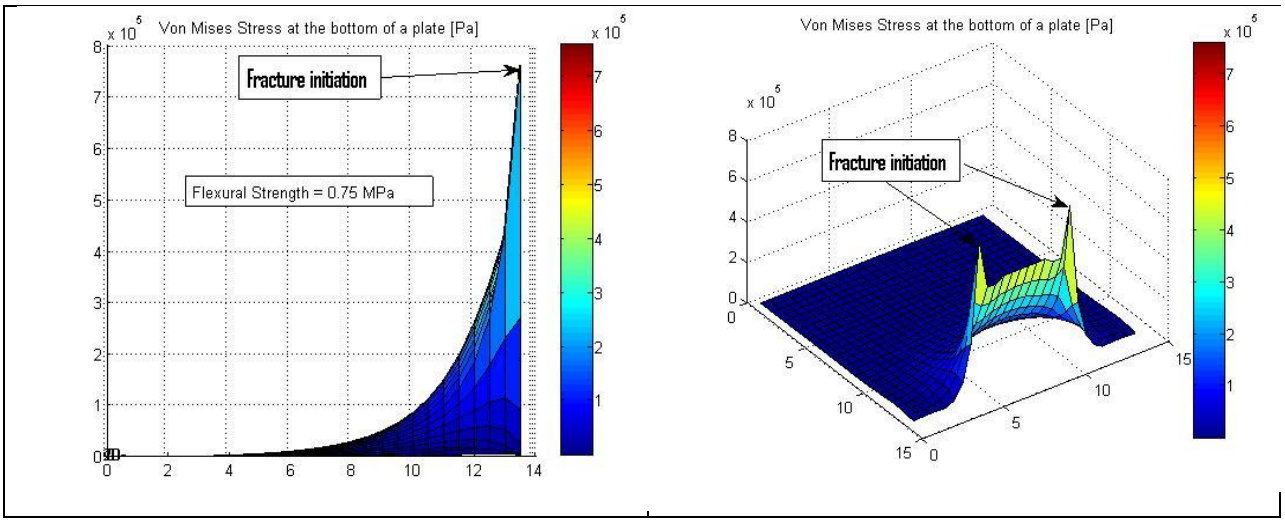

Figure 4.3: Results of the numerical model in terms of Von Mises for contact width of 2 metres

An interesting fact has been observed from the numerical model results that for wedged beam failure mode the force required increases fast with increasing of contact width, while for the plate mode the force required increases slowly (see **Table 4.2**).

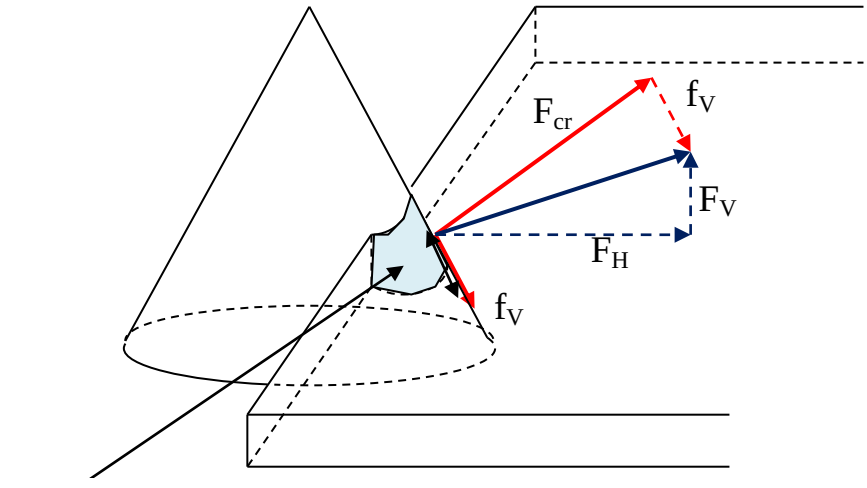

Figure 4.4: Forces arrangement - Sketch for local crushing area during ice-cone interaction

Then we calculate the vertical force corresponding to the crushing event at contact area (see **Figure 4.4**).

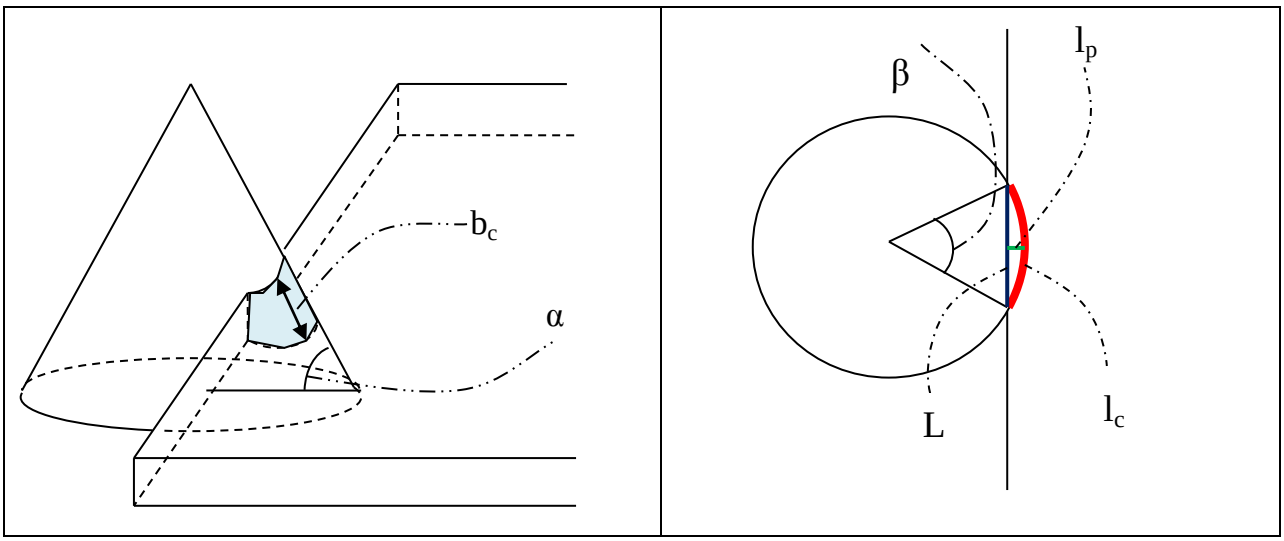

Figure 4.5: Sketch for interaction between an ice sheet and cone

The crushing force is given as:

$$F_{cr} = \sigma_{cr} \cdot A \tag{4.28}$$

The area of contact is calculated by:

$$A = l_c \cdot b_c \tag{4.29}$$

$$L = D \cdot \sin\frac{\beta}{2} \tag{4.30}$$

From this:

$$\beta = 2\arcsin\frac{L}{D} \tag{4.31}$$

$$l_c = R \cdot \beta \tag{4.32}$$

Penetration length of an ice sheet can be found as (**Figure 4.5**):

$$l_p = R(1 - \cos\frac{\beta}{2}) = \frac{D}{2} \cdot (1 - \cos(\arcsin\frac{L}{D})) \tag{4.33}$$

Then,

$$\begin{cases} b_c = \dfrac{h}{\sin\alpha}, if\ l_p \geq \dfrac{h}{\tan\alpha} \\ b_c = \dfrac{l_p}{\cos\alpha}, otherwise \end{cases} \tag{4.34}$$

Thus,

$$A = D\arcsin\frac{L}{D} \cdot b_c \tag{4.35}$$

$$F_{cr} = \sigma_{cr} \cdot D\arcsin\frac{L}{D} \cdot b_c \tag{4.36}$$

The friction force is found as:

$$f_V = \mu \cdot F_{cr} \tag{4.37}$$

And finally, the vertical force is (**Figure 4.4**):

$$F_V = F_{cr} \cdot \cos\alpha - f_V \cdot \sin\alpha = \sigma_{cr} \cdot D\arcsin\frac{L}{D} \cdot b_c \cdot (\cos\alpha - \mu\sin\alpha) \tag{4.38}$$

Now we plot the vertical force required for ice breaking and the vertical force associated with local crushing in one graph and by means of "nodal analysis" determine the contact width. The plot obtained is illustrated in **Figure 4.6**. Parameters for the plot are presented in Table.

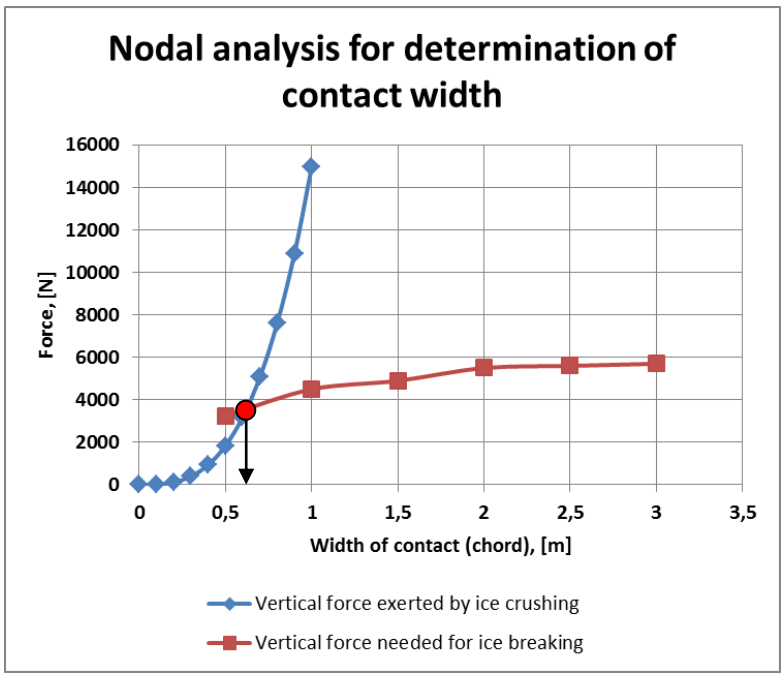

Figure 4.6: "Nodal analysis" for determination of contact with (D=4.5 m)

Property	***Situation 1***	***Situation 2***
Compressive strength	2 MPa	2 MPa
Ice thickness, h	0.1 m	0.1 m
Cone diameter at the ice level, D	4.5 m	2.5 m
Friction coefficient, μ	0.4	0.4

As can be seen from the **Figure 4.6**, the contact width for the situation 1 (structure's diameter at ice level is 4.5 metres) is only about 0.65 metres. Then we implemented the same procedure for the structure's diameter at ice level of 2.5 metres (situation 2). The results of nodal analysis are plotted in **Figure 4.7.**

Contact width (chord)	Vertical force corresponding to failure in bending
0.5 [m]	3.5 [kN] (wedged beam)
1 [m]	4.6 [kN] (wedged beam)
1.5 [m]	6 [kN] (wedged beam)
2 [m]	6.7 [kN] (circumferential)
2.5 [m]	6.5[kN] (circumferential)

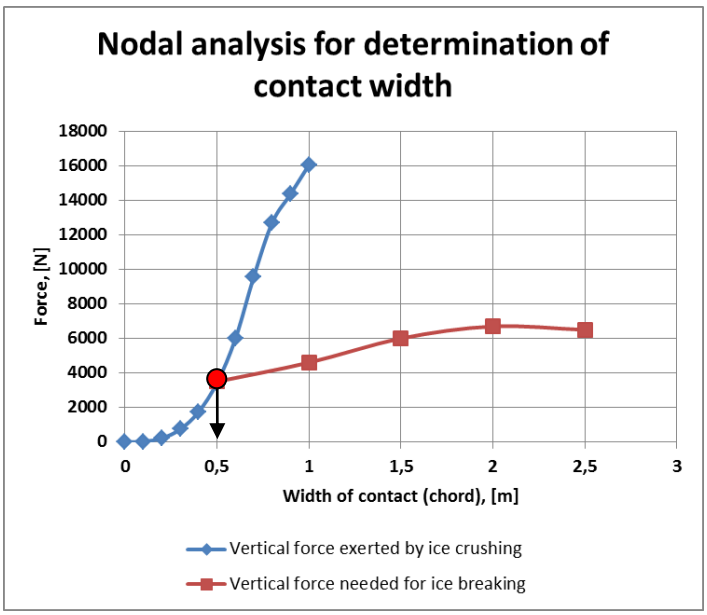

Figure 4.7: "Nodal analysis" for determination of contact with (D=4.5 m)

From **Figure 4.7** we find the contact width for the structure's diameter at ice level of 2.5 metres. The contact width is equal to 0.5 metres. Due to the limitations of mesh size of the model, for both cases we assume the contact width of 0.5 m. The difference for the two cases is the width of wake behind the cone – for the second situation due to bigger diameter it is assumed to be 5.5 metres, while for the first case – 3.5 metres (0.5 metres from the cone to both sides).

After determination of the contact width we can identify failure modes. The results of the simulation in terms of Von Mises stress are presented in Figure 4.8 and Figure 4.9

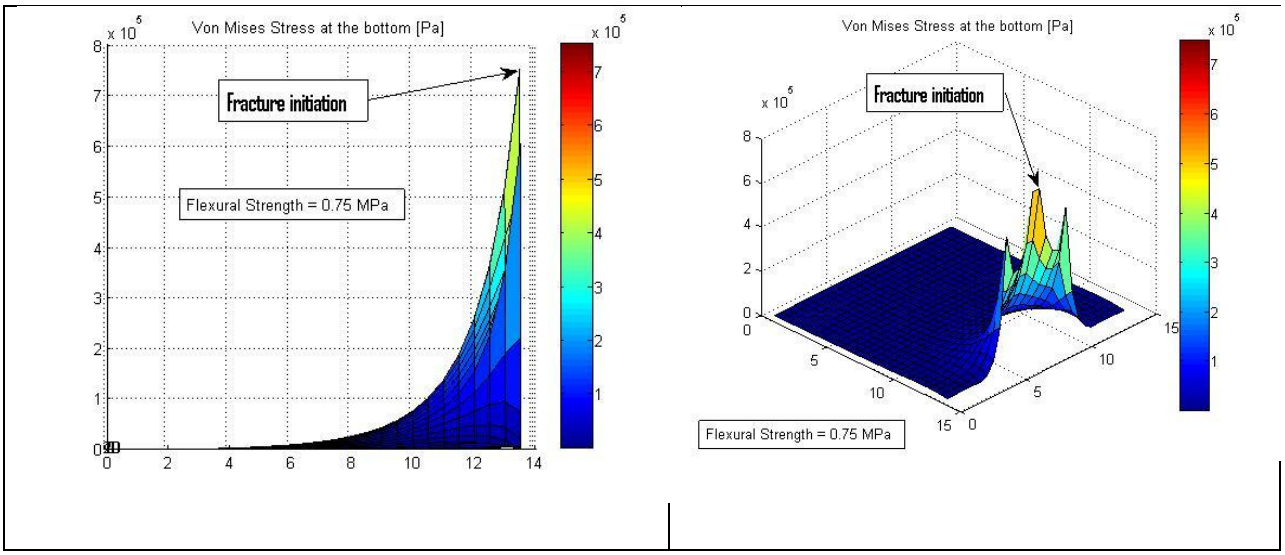

Figure 4.8: Simulation for D/h=25 in terms of Von Mises stress

Plate deflection for these two states are illustrated in Figure

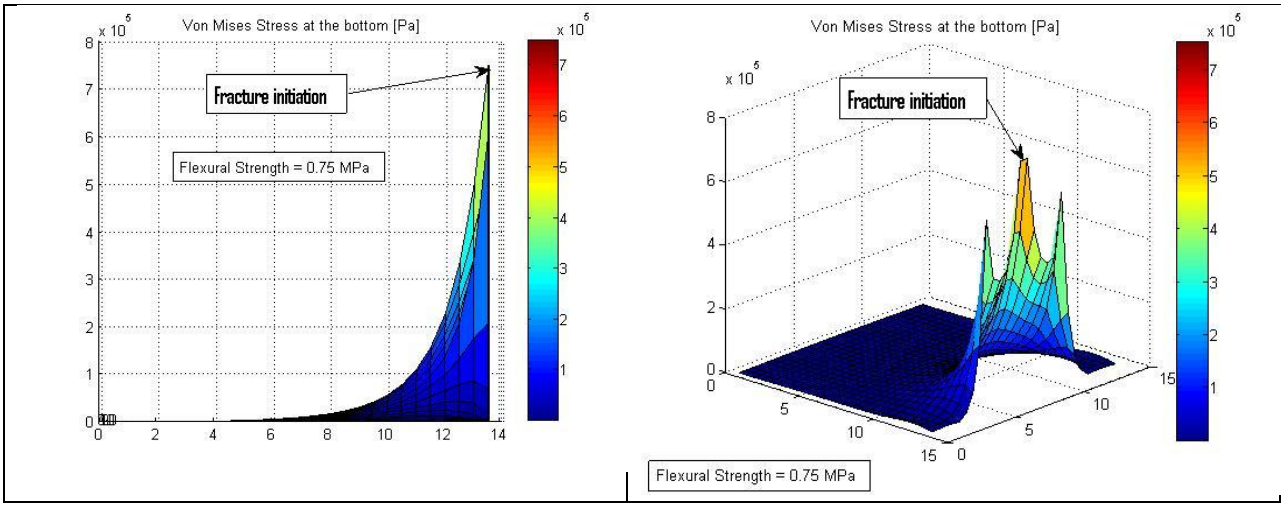

Figure 4.9: Simulation for D/h=45 in terms of Von Mises stress

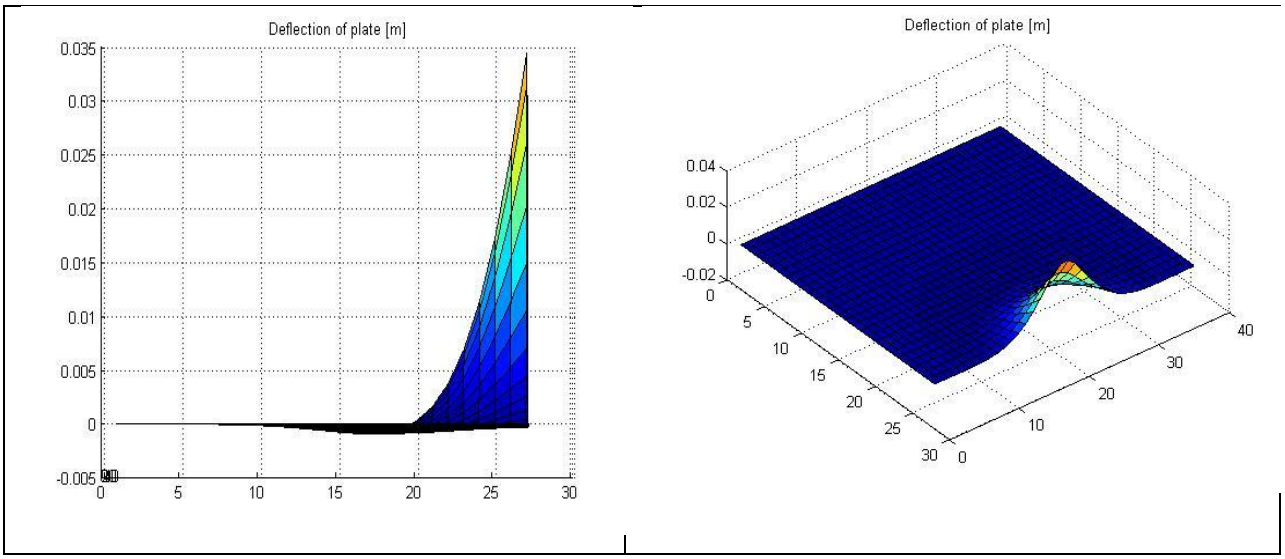

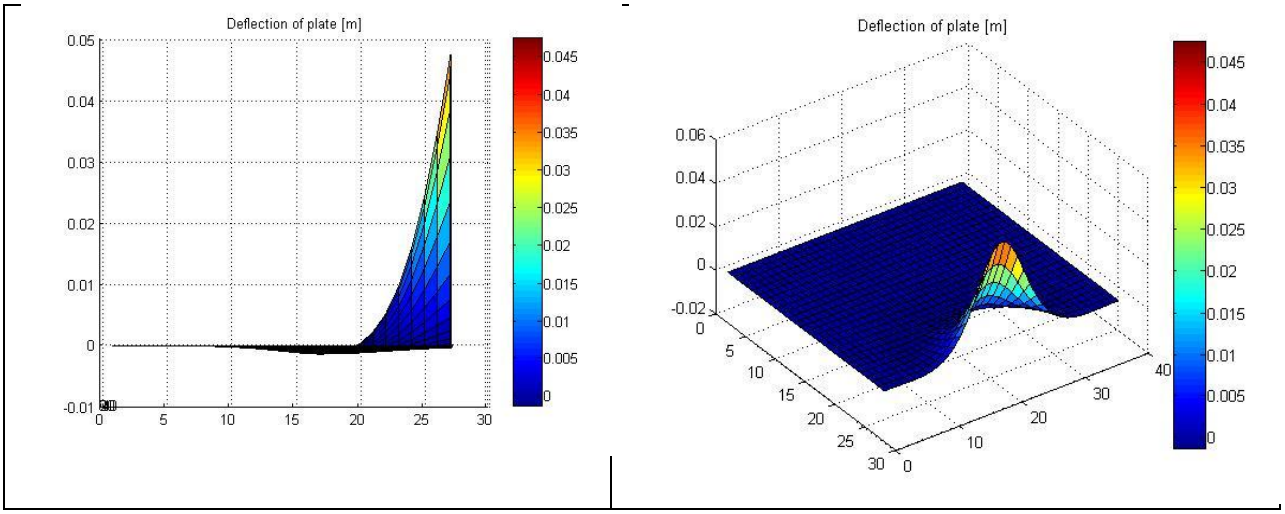

Let us describe the situation with D/h=25 first. As stated by Li et al. (2003) in this state wedged beam failure mode was observed (see **Figure 4.1**). This means that firstly crack initiated near the structure and then propagated radially. Looking at Figure 4.8 one can see that the model

results are in good agreement with the field observation. Figure 4.8 shows that the maximum Von Mises stress occurs at the contact with structure.

Now let us consider the situation when D/h=45 (situation 2). In this state the field observation indicated plate failure mode. However, according to the model results (see Figure 4.9) wedged beam failure still dominates. So, we observe some discrepancy between numerical model and field results. Then in order to identify the discrepancy between model prediction and real data let us find such contact width when the numerical model will indicate plate bending mode. Increasing the width of the contact (D) and analyzing the failure mode predicted we have obtained that with the width of contact of 1.5 metres the numerical model predicts plate bending mode (circumferential crack) (see Figure).

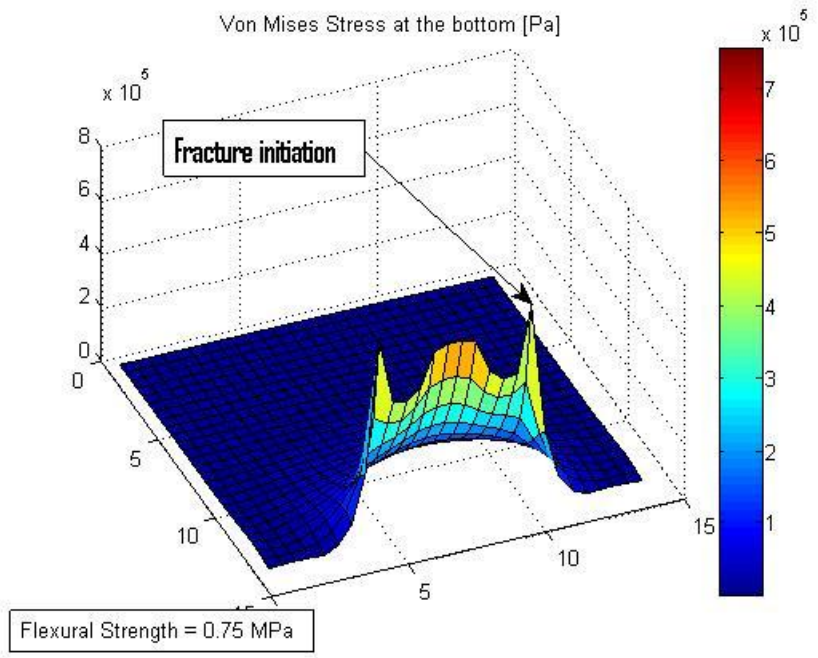

As can be seen from Figure the Von Mises stress no longer reaches the ice flexural strength at the contact with structure, but it occurs at the edge of wake behind the structure. It indicates that a crack forms in some distance from the structure and propagates circumferentially. So, the plate failure mode dominates.

Basing on field observations, Li et al. (2003) gathered statics of failure modes with varying ice level (Figure)

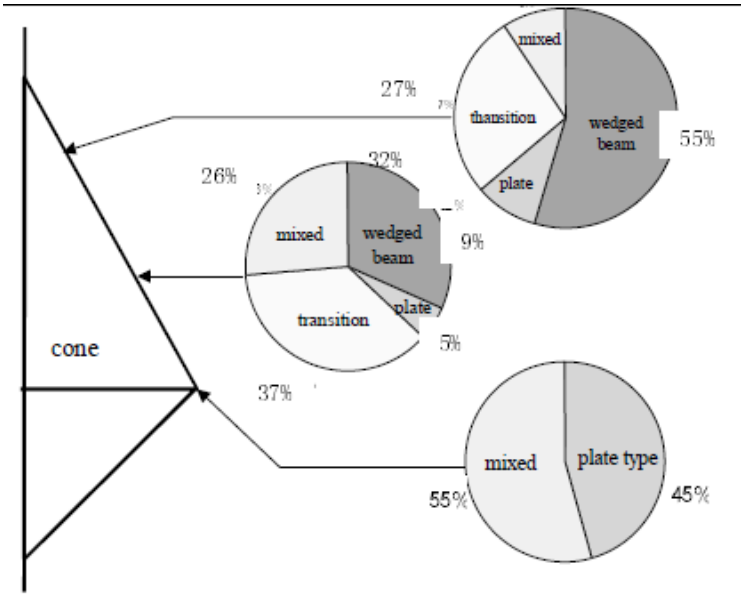

From this statistics it is clearly seen the plate failure mode was observed practically only in the cases of interaction with the base of the cone. In other situations this type of failure occurred very rarely. Li et al. (2003) also state that during tide process both ice drift velocity and the cone diameter are increasing. This means that the ice rubble accumulation increasing the contact width is likely to occur. It can explain the discrepancy of the results obtained by the numerical model. For upper parts of the cone the model results are in agreement with field data and the wedged beam failure mode is predicted.

Summary

The numerical model developed permits determination of bending failure mode. The mode of failure is considered to be of great importance in determination of ice breaking length. It is confirmed by field observations that different failure modes produce different values of ice breaking length. Therefore, this capability of the model is essential for the problem considered in the thesis.

Comparison of the numerical results with field data has shown good agreement in determination of ice failure mode. However, for the base of cone the simulation predicts wedge beam failure mode, while field observations indicate plate mode dominance. These results are explained by relatively narrow contact width (0.65 m) of an ice sheet with a cone obtained by the nodal analysis. The simulation has shown that in our particular problem the plate failure mode dominates in the case of contact width of 1.5 metres. So, the discrepancy can be explained by ice rubble accumulation in front of the cone. For upper parts of the cone both numerical model and field data indicate the dominance of wedged beam failure mode.

4.4. Determination of ice failure load

According to the assumption of Su et al. (2009), before bending failure the local ice crushing occurs up until the moment when the vertical force is sufficient to break the ice sheet in bending. So, the horizontal force exerted on the structure is steadily increasing until the moment of bending failure. This process has been repeatedly confirmed by number of model tests.

Therefore, the vertical force required to break an ice sheet controls horizontal force exerted on the structure.

Kashtelian, referred by Su et al. (2009), assumes that the failure load for an ice edge of opening θ is given by:

$$P_f = C_f(\frac{\theta}{\pi})^2 \sigma_f h_i^2 \tag{4.39}$$

where C_f is an empirical parameter. However, the values of this parameter offered by different authors vary in wide range. Thus, for example, Kashtelian proposed quite small value of about 1, while Nguyen et al. (2009) used the value of 4.5 and validated it by empirical ice breaking formula (Su et al., 2009). Su et al. (2009) for their ice breaking simulation used the value $C_f = 3.1$. Aksnes (2011) in his simplified numerical model used the failure criterion of elastic beam.

Consequently, there is a significant discrepancy between estimations of vertical force required for the ice sheet breaking. Therefore, our attempt here is to estimate failure load by means of the numerical model developed. For this purpose we apply some simplification. Basing on observation of Zhou et al. (2012) made during model tests of icebreaking tanker performance in level ice (see Figure 4.11. Model test study of ship performance in ice (Zhou et al., 2012)Figure 4.11), we assume that the interaction occurs along the sides of the bow as illustrated in Figure 4.10: Simplification of interaction area.

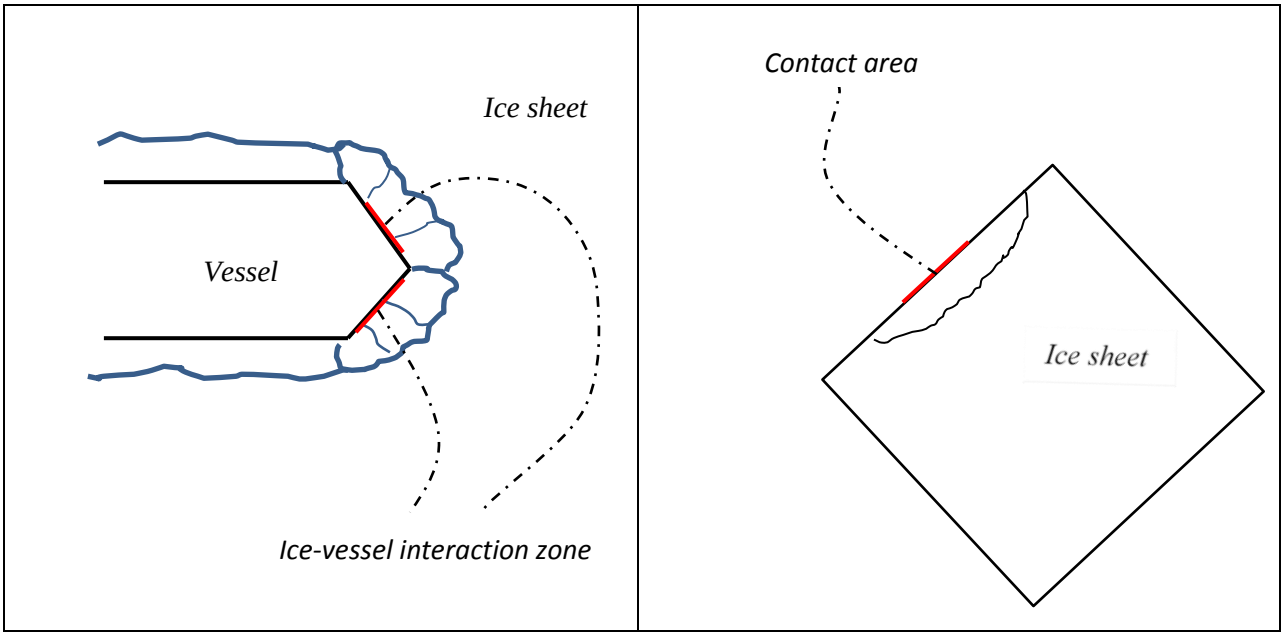

Figure 4.10: Simplification of interaction area

As can be evidently seen from Figure 4.11 (rigth), circumferential cracks right and left of the vessel form almost independently on each other. Therefore we can formulate simulation domain as shown in Figure 4.10. It has to be mentioned that the simplification here is neglecting of boundary effects, since in reality the edge of contact in front of the vessel is not free. But analyzing Figure 4.11, due to intensive failure at the bow tip we believe that this assumption is acceptable.

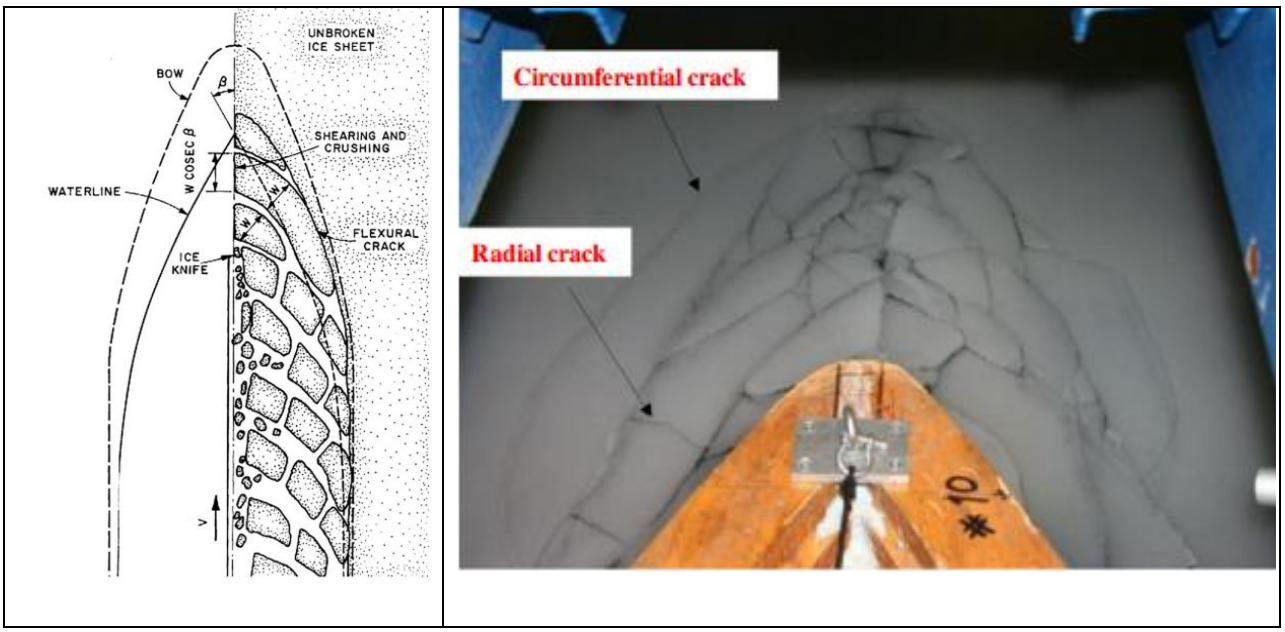

Figure 4.11. Model test study of ship performance in ice (Zhou et al., 2012)

Now with assumptions and simplifications described above, by means of the numerical model developed we evaluate failure load for varying contact width and ice thickness. The procedure of failure load determination consists in increasing vertical load on the ice sheet up until a failure criterion is satisfied (when surface stress exceeds flexural strength). The results in terms of total failure loads and distributed failure loads are presented in Figure 4.12.

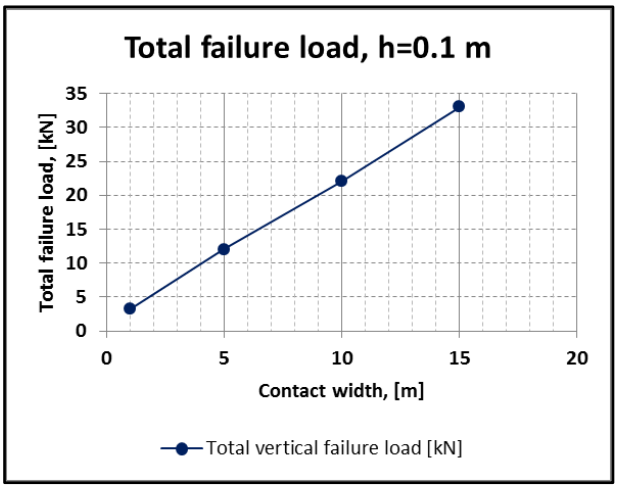

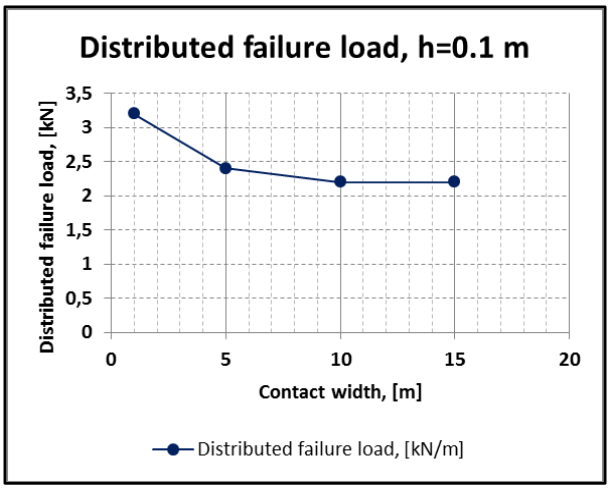

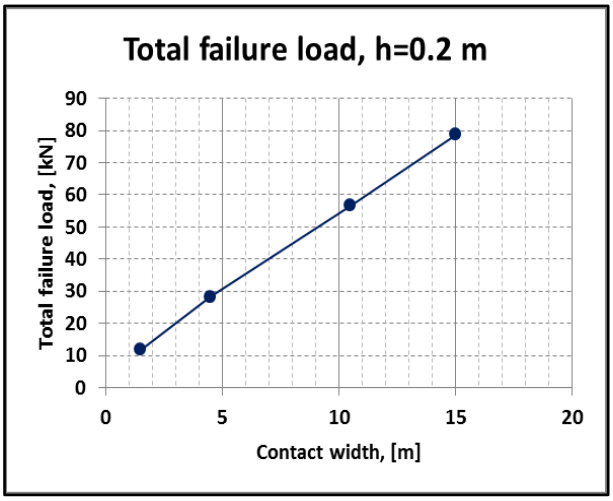
Total failure load, h=0.2 m
Total failure load, [kN]
90
80
70
60
50
40
30
20
10
0
0
5
10
15
20
Contact width, [m]

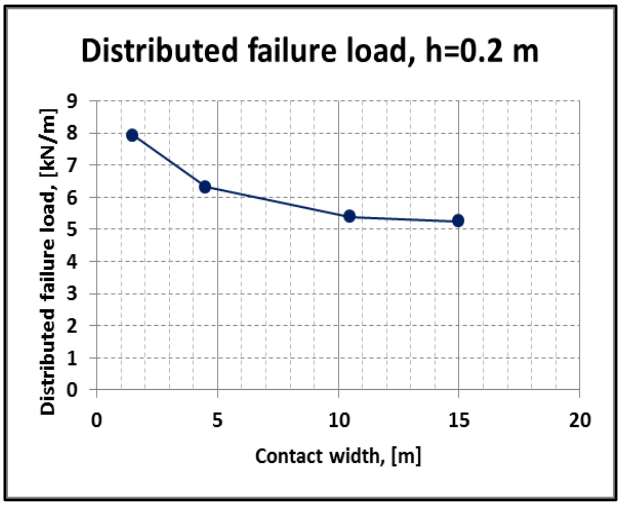
Distributed failure load, h=0.2 m
Distributed failure load, [kN/m]
9
8
7
6
5
4
3
2
1
0
0
5
10
15
20
Contact width, [m]

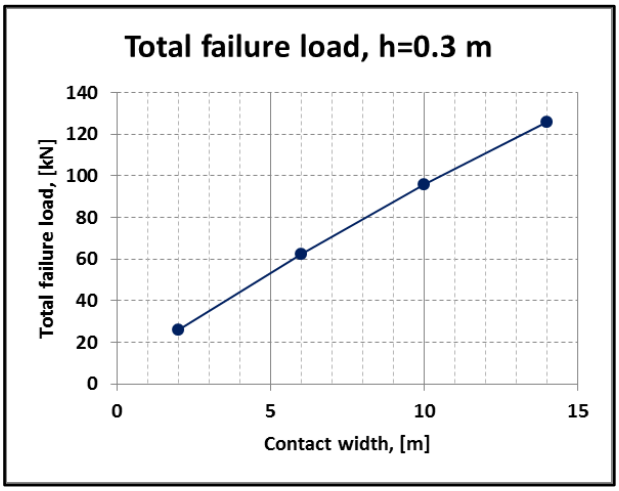
Total failure load, h=0.3 m
Total failure load, [kN]
140
120
100
80
60
40
20
0
0
5
10
15
Contact width, [m]

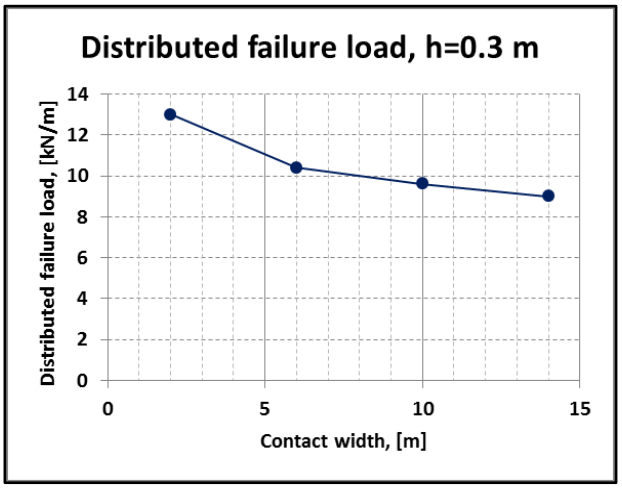
Distributed failure load, h=0.3 m
Distributed failure load, [kN/m]
14
12
10
8
6
4
2
0
0
5
10
15
Contact width, [m]

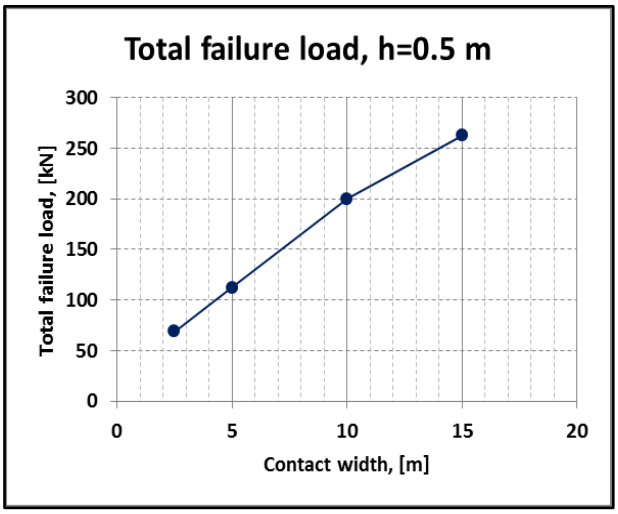
Total failure load, h=0.5 m
Total failure load, [kN]
300
250
200
150
100
50
0
0
5
10
15
20
Contact width, [m]

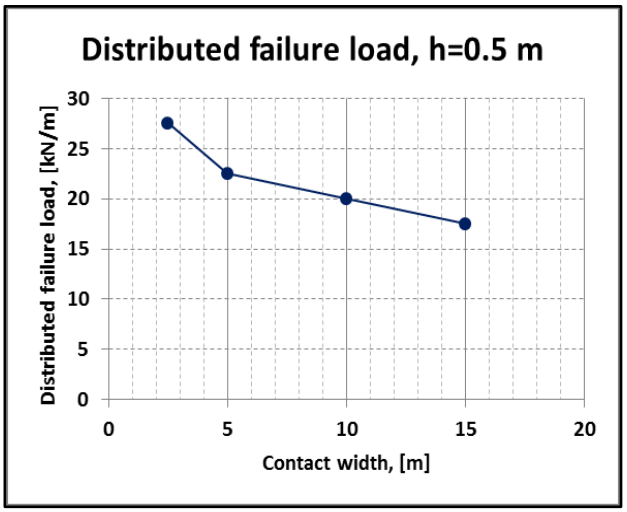
Distributed failure load, h=0.5 m
Distributed failure load, [kN/m]
30
25
20
15
10
5
0
0
5
10
15
20
Contact width, [m]

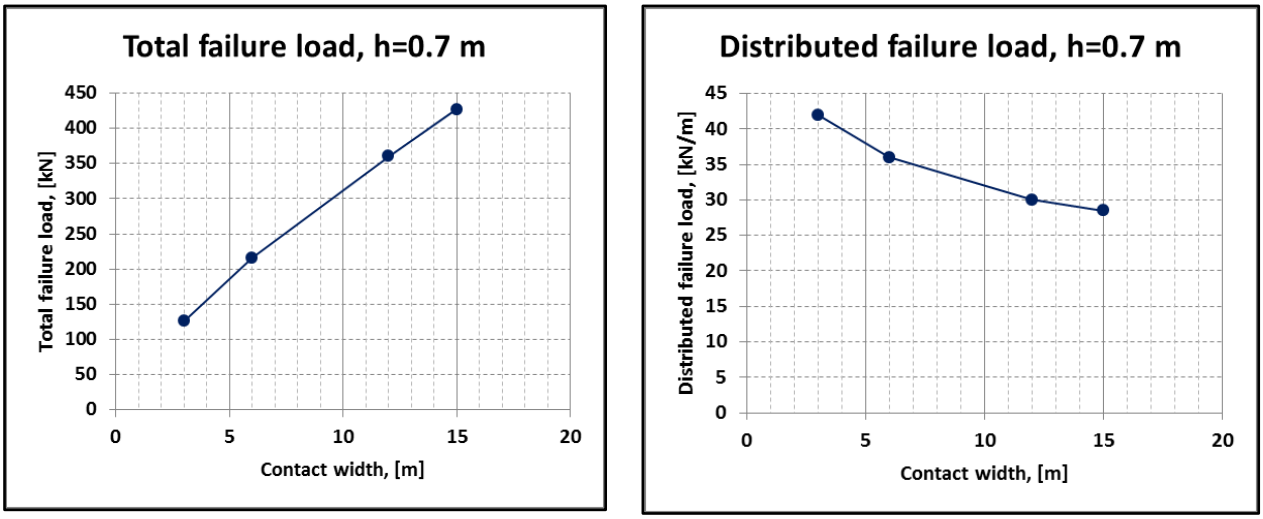

Figure 4.12: Total and per unit length ice failure loads obtained by the numerical model

An important observation can be made from the results obtained. Looking at the distributed failure load one can notice that it decreases hyperbolically and approaches a constant value. This means that the failure occurs at the same distributed load regardless of the contact width. Consequently, lateral bending of an ice sheet does not contribute to the picture any more. It means that the loaded width of an ice sheet is no more important and therefore the ice sheet can be treated as an elastic beam. So, according to the classification given by Lau et al. (1999) the semi-infinite failure mode dominates.

Summary

The failure load is essential parameter for ice-structure interaction since it governs the magnitude of the horizontal load on the structure. For our particular problem of ice - moored vessel interaction we applied a simplification that the interaction occurs along bow's sides independently. With this assumption by means of the numerical model developed the failure loads are calculated for different contact widths and ice thicknesses. These results will be further used as input parameters for the problem of FPSO surge motion.

It is worth mentioning that the results of failure loads revealed an interesting fact that the distributed load decreases hyperbolically and approaches a constant value at certain contact width. Therefore, the model allows prediction of transition to semi-infinite beam failure mode.

CHAPTER 5: NUMERICAL SIMULATION OF FPSO BEHAVIOUR IN LEVEL ICE

5.1. General

Due to less resistance to the ice action, FPSO units operating in ice environment require ice management. However, FPSO operation in harsh Arctic environments can be faced with the situations significantly reducing the efficiency of the ice management. For instance, ice drift can fast change its direction. The direction of the ice drift can be changed to opposite one in merely half an hour (Løset et al., 2001) (**Figure 5.1**). Another factor that can significantly influence the efficiency of ice management is high ice drift velocity. The situation can further be aggravated by low visibility due to darkness and fog. Also an encroachment of large ice features such as ice ridges or icebergs may require immediate ice management measures leaving FPSO to interact with less dangerous level ice. Consequently, though ice management is implemented, FPSO interaction with level ice or with a big ice floe is quite a probable situation and should be taken into consideration. Therefore, floating production units intended for operation in ice environment have to be properly designed for interaction with level ice.

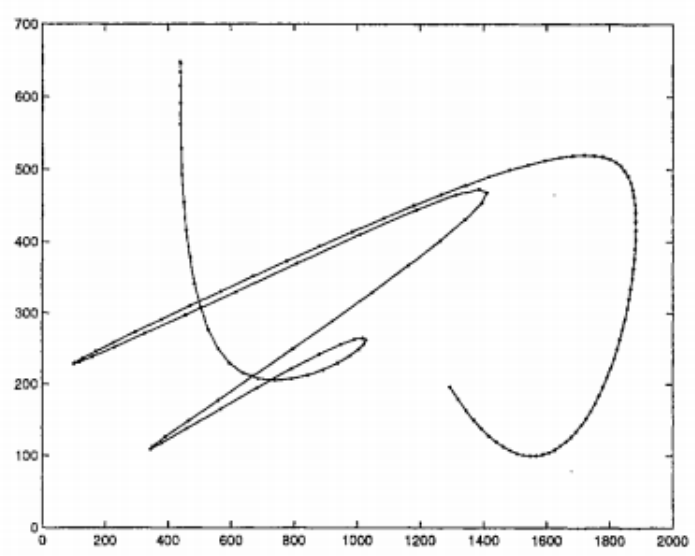

Figure 5.1. Modelled movement of the ice drift. Dots every 10 minutes (Løset et al., 2001)

Two major problems of interaction between a floater and an ice sheet are believed to be loads on the hull and the mooring loads. In this chapter our attention is limited to consideration of the particular problem of mooring loads.

It can be evidently noticed that the FPSO surge motion in level ice generally resembles an icebreaker performance. In the first case the level ice advances towards the vessel, while in the second case an icebreaker advances towards the level ice. So, generally the interaction process is the same. Therefore, Zhou et al. (2011) in the simulation of moored structure station keeping in level ice has based on ideas of Su et al. (2009), who investigated icebreaking ship performance in level ice.

5.2. Review of the main ideas used for simulation of FPSO surge motion in level ice

Su et al. (2009) has developed the numerical model to simulate ship maneuvers in level ice. The attribute of the model developed by Su et al. (2009) is that it is capable to simulate continuous ice breaking process, while early research on level ice resistance was usually based on break-displace process (see **Figure 5.2**).

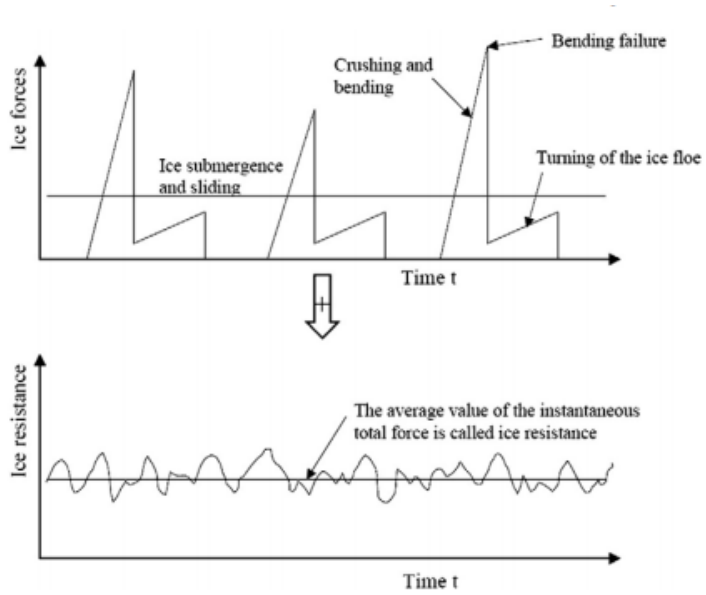

Figure 5.2. Idealized time histories of ice forces (upper: break-displace process approach, lower: continuous ice breaking) (Riska, 2007 cited by Su et al., 2009)

The approach of Su et al. (2009) is based on the discretization of an ice sheet and a hull into a number of nodes (**Figure 5.3**). When an ice node is found inside the hull polygon, the contact is considered to be detected. After the contact is detected the ice wedge is involved in break-displace process. It is assumed that in the first stage a local ice crushing occurs at the contact area. The crushing keeps growing with an increasing contact area until its vertical component is sufficient to break an ice sheet in bending. The bending length in the model of Su et al. (2009) is characterized by single parameter – icebreaking radius R (illustrated in **Figure 5.3** by red dots). Such a way, as seen from **Figure 5.3** non-simultaneous ice breaking process is simulated.

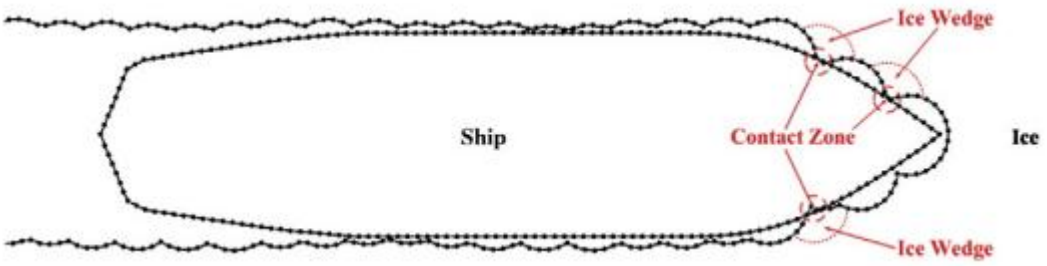

Figure 5.3. Discretization of ship hull and ice edge into a number of nodes (Su et al. 2009)

The model of Su et al. (2009) implies that the interaction between ship and level ice takes place in several phases. Firstly, ice crushing occurs up until the bending failure of ice (breaking phase), then the ship forces broken ice floes to turn on edge until parallel to the hull (rotation

phase), then the submerged floes slide along the hull (sliding phase). These three phases involved in the ice breaking process are proposed by Kotras et al. (1983) (Aksnes, 2011).

For the rotation phase the main influencing parameters are the mass and dimensions of a broken floe, ice-hull friction coefficient and relative velocity between ice and ship. In turn, for the sliding phase the governing parameters are ice-hull friction coefficient, relative velocity between the ship and drifting ice and the ice-hull contact area. Finally, the loads during the breaking phase mainly depend upon the ice thickness, compressive strength of ice, hull geometry (angles of inclination) and the failure load.

As already mentioned in Chapter 4, there are many discrepancies in failure load estimation. Su et al. (2009) in their simulation used the formula for failure load introduced by Kashtelian (Su et al., 2009):

$$P_f = C_f(\frac{\theta}{\pi})^2 \sigma_f h_i^2 \tag{5.1}$$

The value of 3.1 for C_f coefficient was used in the modelling and it was argued that this value gives reasonable mean ice breaking force as compared to the Lindqvist's ice resistance (Su et al., 2009). However, it is important to mention that the formula (5.1) presented above has empirical nature, and so it does not have mathematical or physical foundation. Therefore, the empirical coefficient C_f may vary for different cases and this formula may not always be valid.

The numerical model developed by Su et al. (2009) was validated by comparison with field data from the ice trials of icebreaker Tor Viking II and fairly good agreement has been achieved.

Another numerical model of moored vessel behaviour in level ice has been developed by Aksnes and Bonnemaire (2009). The ice breaking cycle is two-dimensional. The surge motion of a moored ship is only considered. Aksnes and Bonnemaire (2009) states that the surge motion is often the dominant mode of motion for a moored ship-shaped vessel.

In the simplified model of Aksnes and Bonnemaire (2009) the ice sheet is treated as an elastic beam with randomness in mechanical ice properties, ice thickness and ice breaking length. The failure load corresponds to elastic beam failure in bending (when the stress at the upper surface exceeds the flexural strength of ice). Since the flexural strength of ice is calculated from the temperature and salinity, which are assumed random in prescribed distribution, the failure load is varying. Ice thickness and ice breaking length are also determined from the prescribed distribution. The numerical model of Aksnes and Bonnemaire (2009) does not take ice crushing into account and the horizontal force exerted to the structure is calculated as for elastic beam. The process of ice-hull interaction also includes three main phases, namely ice breaking, rotation and sliding.

The results of simulation have revealed a number of nonlinear coupling effects between vessel response and ice forces at low speed of ice drift.

Zhou et al. (2011) have developed a two-dimensional numerical model of moored vessel behaviour in level ice with three degrees of freedom (surge, yaw and sway). The principles of the model are mainly based on the ideas of Su et al. (2009). The model is intended to simulate time

history of ice forces, global mooring forces and dynamics of a moored floating structure. The numerical model was validated by comparison with real field data obtained for Kulluk platform and has shown fairly good agreement.

5.3. Description of the numerical model of FPSO surge motion in level ice

The numerical model for investigation of FPSO behaviour in level ice developed in this thesis is chiefly based on ideas of Su et al. (2009), Aksnes and Bonnemaire (2009) and Zhou et al. (2011). However, our attempt here is to contribute to the knowledge about proper determination of ice sheet's failure load, which is known to be one the most influencing parameter on the ice-ship interaction. Another novelty of the model developed within the thesis is consideration of ice-hull friction coefficient varying with relative velocity. This phenomenon explains the fact of ice load increase when ice drift velocity is low, which was observed during the model test carried out by Aksnes (2010).

In the models of Su et al. (2009) and Zhou et al. (2011) the bending failure is assumed to occur when the vertical component of force F_V reaches the failure load P_f given by formula (5.1). However, the empirical coefficient C_f is unknown and recommendations for this coefficient vary in wide range (Kashtelian recommended $C_f \approx 1$, Nguyen – C_f =4.5, Su et al. (2009) – C_f =3.1). It can also be noticed that the failure load given by formula (5.1) by no means depends upon the contact width, which may seem to be quite questionable. The results of the numerical simulation of ice sheet bending developed in this work and presented in Chapter 4 have evidently shown that the failure load increases with increasing of the contact width (Figure 4.12). Therefore, the formula (5.1) for the failure load seems to be valid only for ice wedges, i.e. when the contact width is small. However, from the model test of icebreaking tanker performance in level ice carried out by Zhou et al. (2012) one can observe that the ice-hull contact area can be wide (e.g. see Figure 4.11).

In the model of Aksnes and Bonnemaire (2009) the failure load is assumed as for an elastic beam.

Therefore, in our numerical model we use the failure load obtained by the numerical simulation of ice sheet bending (see Chapter 4).

Let us now describe the principles of the numerical model of FPSO surge motion in level ice.

The governing equation for FPSO surge motion in level ice can be formulated as:

$$(M + M_a)\frac{d^2x}{dt^2} = R_b + R_{rot} + R_s + F_m + F_{ow}$$

where R_b – ice breaking horizontal force;
R_{rot} - rotation force;
R_s – sliding force;
F_m – mooring force;
F_{ow} – hydrodynamic force;
M_a – added mass;[

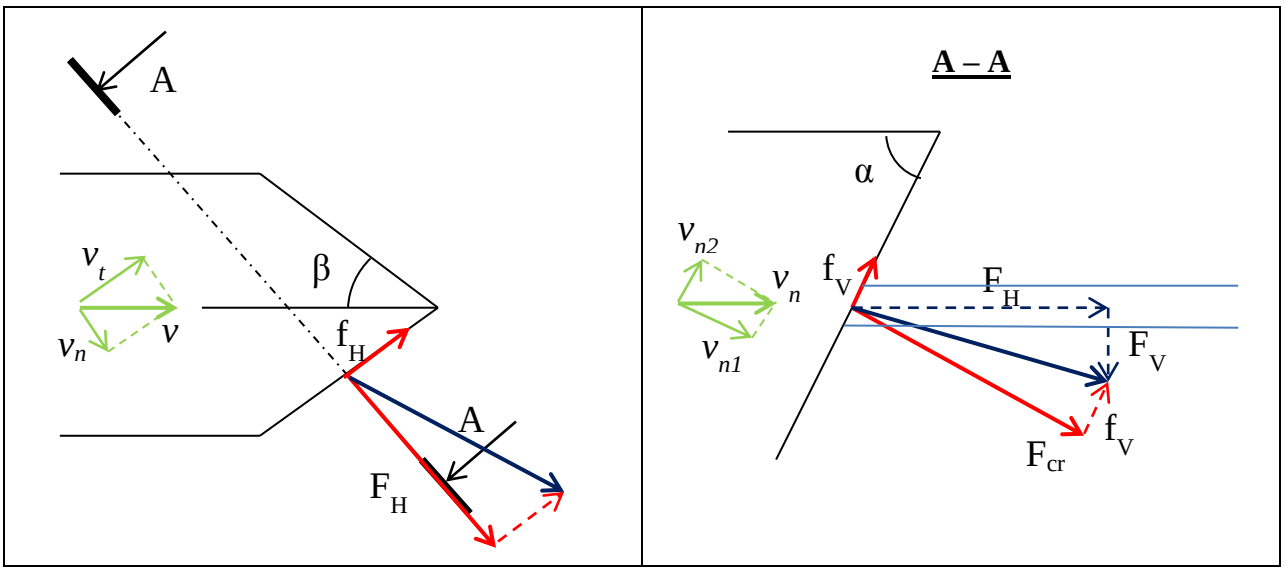

Figure 5.4: Sketch on ice breaking force determination

Horizontal ice breaking force

In order to find horizontal ice breaking force we follow the ideas of Su et al. (2009) who assumed that the local crushing occurs at the contact up until the vertical force is sufficient to break an ice sheet in bending. The criterion for ice sheet failure in bending is described in Chapter 4. Let us find the vertical force.

The crushing force can be found as:

$$F_{cr} = \sigma_c \cdot A$$

The contact area A is found as:

$$A = l_c \cdot b_c$$

where l_c is a contact width.

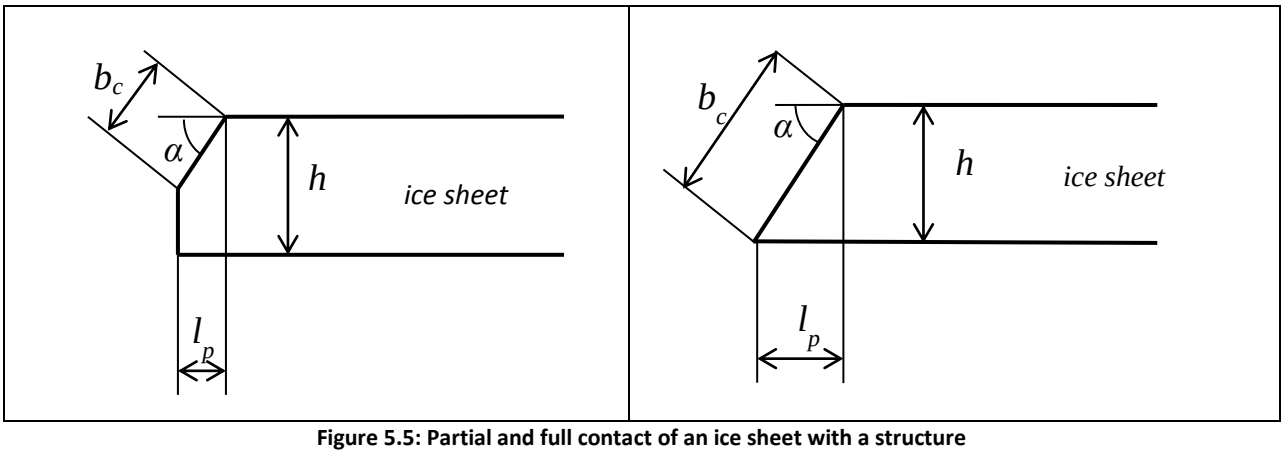

Figure 5.5: Partial and full contact of an ice sheet with a structure

Looking at Figure 5.5, b_c can be found as:

$$\begin{cases} b_c = \dfrac{l_p}{\cos\alpha}, if\ l_p \le \dfrac{h}{\tan\alpha} \\ b_c = \dfrac{h}{\sin\alpha}, otherwise \end{cases}$$

where $l_p = x_{sh} - x_{ice}$ is penetration length of a ship into the ice.

The components of friction force are given as:

$$f_V = \mu \cdot F_{cr} \cdot \frac{v_{n1}^{rel}}{\sqrt{(v_{n1}^{rel})^2 + (v_t^{rel})^2}}$$

$$f_H = \mu \cdot F_{cr} \cdot \frac{v_t^{rel}}{\sqrt{(v_{n1}^{rel})^2 + (v_t^{rel})^2}}$$

where v_{n1}^{rel} and v_t^{rel} are components of relative velocity between ice and a ship (see Figure 5.4).

Then, the vertical force is calculated as:

$$F_V = F_{cr} \cdot \cos\alpha - f_V \cdot \sin\alpha$$

If the vertical force F_V exceeds the failure load calculated at Chapter 4, then the failure occurs.

The force component F_H is found by:

$$F_H = F_{cr} \cdot \sin\alpha + f_V \cdot \cos\alpha$$

Then, the horizontal ice breaking force R_b is calculated as follows:

$$R_b = F_H \cdot \sin\beta + f_H \cdot \cos\beta$$

Rotation force

A simplified method to find rotation force is applied in the simulation.

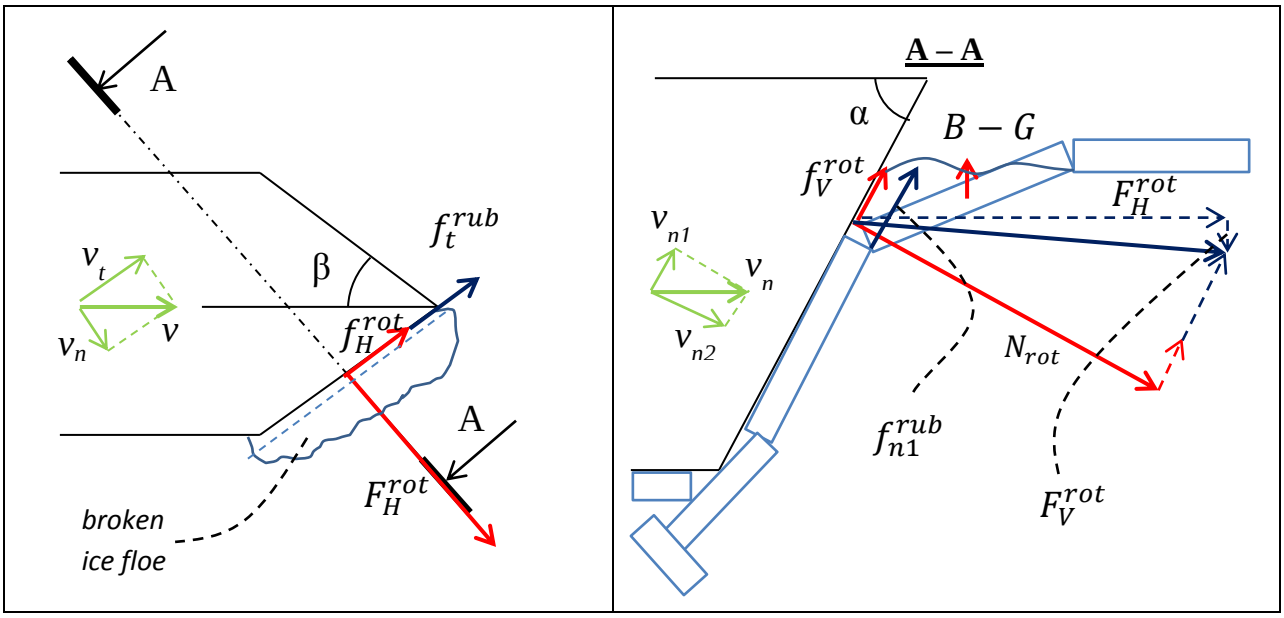

Figure 5.6: On derivation of rotation force

Looking at Figure 5.6, from equilibrium one can find:

$$N_{rot} \cdot \cos\alpha - f_V^{rot} \cdot \sin\alpha - f_{n1}^{rub} \cdot \sin\alpha = (\rho_w - \rho_{ice}) g h \cdot W \cdot l_p$$

where W is an ice breaking length;

l_c is length of broken ice floe;

h is ice thickness;

f^{rub} is a force representing resistance to rotation of the floe due to presence of ice rubble.

The vertical force of the submerged ice pieces parallel to the stem can be found as:

$$B^{rub} = (\rho_w - \rho_{ice}) \cdot g \cdot h \cdot l_p \cdot \frac{T}{\sin \alpha}$$

Then,

$$f^{rub} = \mu \cdot B^{rub} \cdot \cos \alpha$$

$$f_{n1}^{rub} = \mu \cdot B^{rub} \cdot \cos \alpha \cdot \frac{v_{n1}^{rel}}{\sqrt{(v_{n1}^{rel})^2 + (v_t^{rel})^2}}$$

$$f_t^{rub} = \mu \cdot B^{rub} \cdot \cos \alpha \cdot \frac{v_t^{rel}}{\sqrt{(v_{n1}^{rel})^2 + (v_t^{rel})^2}}$$

The components of friction force for rotating ice floe are given as:

$$f_V^{rot} = \mu N^{rot} \frac{v_{n1}^{rel}}{\sqrt{(v_{n1}^{rel})^2 + (v_t^{rel})^2}}$$

$$f_H^{rot} = \mu N^{rot} \frac{v_t^{rel}}{\sqrt{(v_{n1}^{rel})^2 + (v_t^{rel})^2}}$$

$$F_H^{rot} = N^{rot} \cdot \sin \alpha + f_V^{rot} \cdot \cos \alpha + f_{n1}^{rub} \cdot \cos \alpha$$

Finally, we obtain horizontal component of the ice resistance due to rotation:

$$R_{rot} = F_H^{rot} \cdot \sin \beta + f_H^{rot} \cdot \cos \beta + f_t^{rub} \cdot \cos \beta$$

Mooring force

As was shown by Zhou et al. (2011), when vessel's offset is relatively small, the mooring restoring force can be approximated as linear, with certain stiffness. In our model we apply the same simplification. Then the mooring restoring force is given as:

$$F_m = -k \cdot \Delta x$$

where k is mooring stiffness, [kN/m], and Δx is vessel's offset.

Hydrodynamic force

The hydrodynamic forces are represented by drag forces due to vessel's motion relative to water. The drag force is calculated as:

$$F_{ow} = -\frac{1}{2} \cdot \rho_w \cdot C_d \cdot A \cdot \left(v_{ship} - v_{current}\right)^2 \cdot sign(v_{ship} - v_{current})$$

where C_d is drag coefficient,

A is cross-sectional area;

$$sign(v_{ship} - v_{current}) = \begin{cases} 1, if\ v_{ship} - v_{current} > 0 \\ -1, otherwise \end{cases}$$

Ice breaking length

There is a significant discrepancy in determination of ice breaking length. The common way to represent ice breaking length is by its non-dimensional ratio to characteristic length. The latter is given as:

$$l_c = \left(\frac{Eh^3}{12 \cdot (1 - \nu^2)\rho_w g}\right)^{1/4}$$

Thus, for example Heternyi (1946) obtained this non-dimensional value C_l of 0.785 considering simple elastic theory. George (1986) obtained a value of approximately 0.6 based on a plate theory. Frederking (1980) used a wedged beam model and derived a value of approximately 0.8 (Zhou et al., 2012). The results of model tests and full-scale tests significantly vary as well. Zhou et al. (2012) state that Abdelnour and Sayed (1982) obtained a ratio of C_l=0.5 from the model tests of a man-made island in shallow water; Ettema et al. (1987) performed model tests for a polar-class icebreaker and found that C_l is less than unity, ranging from 0.8 to 0.4; Lau et al. (1999) analyzed the breaking length of ice on sloping structures bases on model scale observations, where the value was reduced from 0.7 to 0.1 while the ice thickness was increased on model cone tests and the conversion limit was 0.1. We see that the value of ice breaking length varies in wide range. However, this mainly affects only the frequency of ice-ship contact. In consideration of the fact that the frequency can be compensated by varying ice drift velocity, we believe that this parameter does not have significant influence on mooring loads, being the subject of our investigations.

In our model we assume ice breaking length obtained from the experimental tests of icebreaking tanker performance in level ice carried out by Zhou et al. (2012). They obtained typical average non-dimensional ratio C_l ranged between 0.22 and 0.30. The authors state that the plate type of bending failure was observed and typical ice breaking length of 2-6 times the ice thickness was obtained, which well coincides with typical values for plate failure mode.

Added mass

When the ship is moving, she carries along a portion of water, which creates additional inertia of the system. In our model we assume added mass to be 20% of the total mass of the vessel.

Kinetic and static ice-hull friction coefficient

Frederking and Barker (2002) have implemented model investigation of ice-steel friction coefficient in ice tank. They have revealed that the friction coefficient significantly depends on sliding velocity. Their results of ice friction coefficient interacting with painted steel are presented in Figure 5.7.

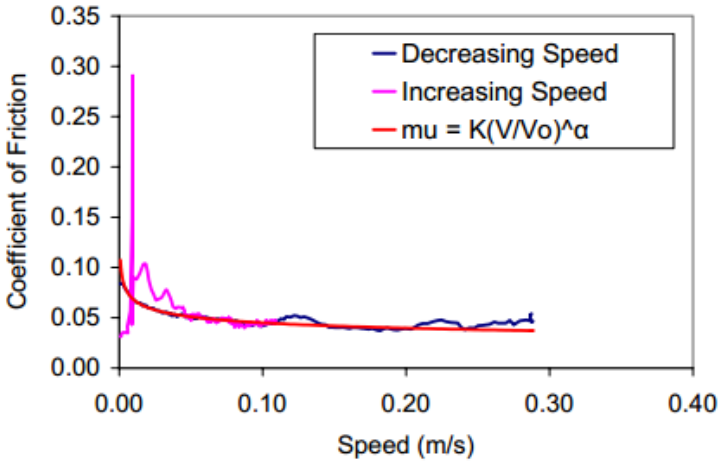

Figure 5.7: Velocity dependent friction coefficient

Frederking and Barker (2002) have obtained that static friction coefficient is much greater than the kinetic one. The authors have also proposed approximation formulae to evaluate friction coefficient:

$$\mu = K \cdot (\frac{v}{v_0})^{\alpha}$$

where K is a friction coefficient at 0.1 m/sec;

v_0 is normalized speed (0.1 m/sec);

α is a constant.

The authors state that for ice interaction with smooth painted steel the values $K = 0.045$ and $\alpha = -0.18$ represent good approximation. The static friction coefficient obtained by the model test for smooth painted steel is about 0.25.

Solution of the equation

The problem is solved by means of time discretization. For each time step the positions of the ship x_{ship} and the ice edge x_{ice} are calculated. If the ice-ship contact is detected, the horizontal ice breaking force is calculated in accordance with formulae presented above. If the vertical force exceeds ice failure load, the ice sheet is assumed to fail and ice edge position is moved back to a certain distance with correspondence to ice breaking length. At each time step the resulting force is determined and ship's acceleration, velocity and position for the next time step are recalculated as follows:

$$a^{j+1} = \frac{R_b^j + R_s^j + F_m^j + F_{ow}^j}{(M + M_a)}$$

$$v^{j+1} = v^j + a^j \cdot \Delta t$$

$$x_{ship}^{j+1} = x_{ship}^j + v^j \cdot \Delta t + \frac{a^j \cdot \Delta t^2}{2}$$

The ice edge position at the next time step is calculated as:

$$\begin{cases} x_{ice}^{j+1} = x_{ice}^{j} - dx_{ice} + v_{ice} \cdot \Delta t, & in\ the\ case\ of\ ice\ sheet\ failure \\ x_{ice}^{j+1} = x_{ice}^{j} + v_{ice} \cdot \Delta t, & otherwise \end{cases}$$

where Δt is time step.

The numerical simulation described above is implemented in MATLAB.

5.4. Results of the numerical simulation of FPSO surge motion in level ice

Verification of the numerical model.

In order to validate the model developed we compare the results with those obtained by model test of moored ship behaviour in level ice carried out by Aksnes (2010) (Aksnes, 2011).

The main parameters of the model test performed by Aksnes are listed in Table 5.1.

Table 5.1: Parameters of the model test performed by Aksnes (2011)

Parameter	Value
Vessel's parameters	
Length, L	106 m
Breadth, B	33 m
Draught, T	8.8 m
Volume displacement, ∇	28,125 m^3
Stem angle, α	25^o
Soft mooring stiffness, k^{soft}	250 kN/m
Stiff mooring stiffness, k^{stiff}	1125 kN/m
Ice properties	
Ice thickness, h	0.75 m
Flexural strength, σ_f	625 kPa
Modulus of elasticity, E	≈1.3 GPa
Ice density, ρ_i	929 kg/m^3

The bow of the model vessel was not sharpened and was flat. Therefore the β angle in Figure 5.4 is equal to 90^o.

Firstly, by means of the numerical model of ice sheet-structure interaction presented in Chapter 4, the failure load is identified. For this purpose, the contact length is assumed to be equal to the vessel's breadth, since the bow is flat. The failure load is found by increasing the force applied at the edge of plate up until the moment when Von Mises stress exceeds the flexural strength of ice (see Figure 5.8). Thus, we have obtained the failure load (the force required to break an ice sheet in bending) equal to 0.99 MN.

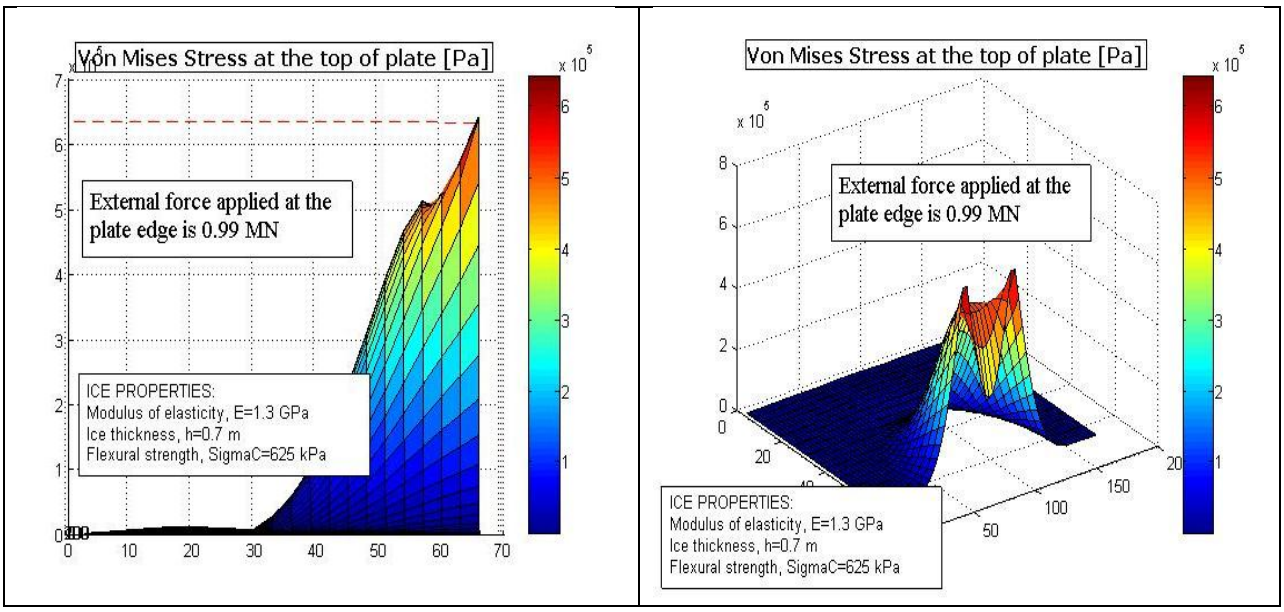

Figure 5.8. Determination of failure load for the simulation of FPSO surge motion

From Figure 5.8 it is seen that the plate failure mode dominates. According to the model test of icebreaking tanker performance in level ice carried out by Zhou et al. (2012), where dominance of plate failure mode was observed as well, for our simulation setup we assume the ice breaking length equal to 2 times the ice thickness.

The setup parameters for four simulation runs are listed in Table 5.2. With the purpose of comparison these parameters correspond to the setup parameters for model tests implemented by Aksnes (2011).

Table 5.2: Setup parameters for the simulation runs

Number of a simulation run	*Mooring stiffness*	*Ice drift velocity*
Run #1	250 kN/m	0.05 m/sec
Run #2	250 kN/m	0.25 m/sec
Run #3	1125 kN/m	0.05 m/sec
Run #4	1125 kN/m	0.25 m/sec

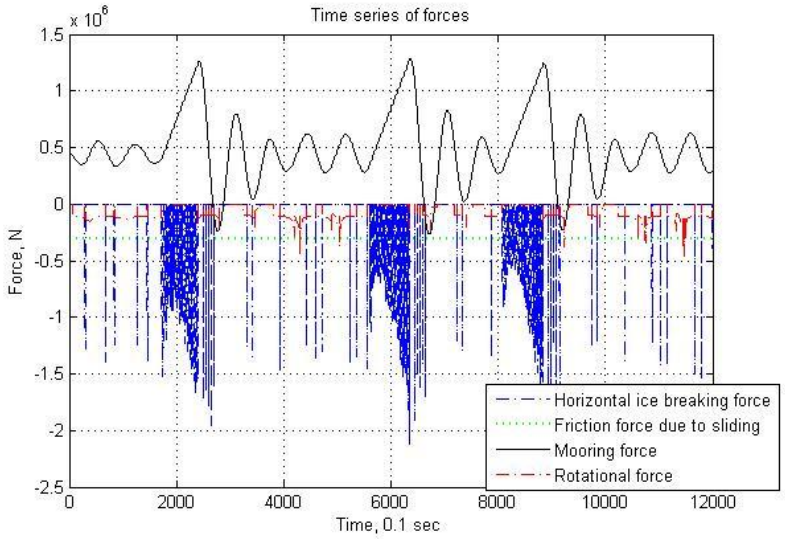

Figure 5.9: Simulation results – k=250 kN/m, v=0.05 m/sec

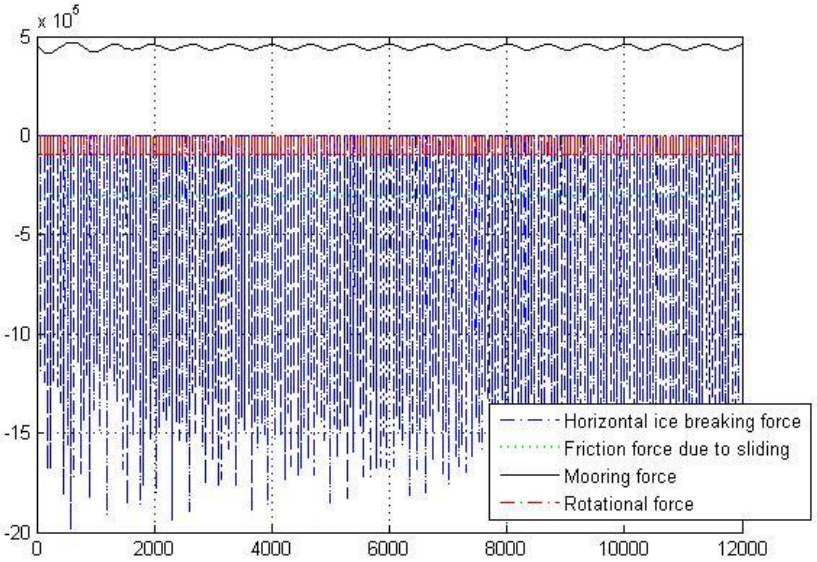

Figure 5.10: Simulation results – k=250 kN/m, v=0.25 m/sec

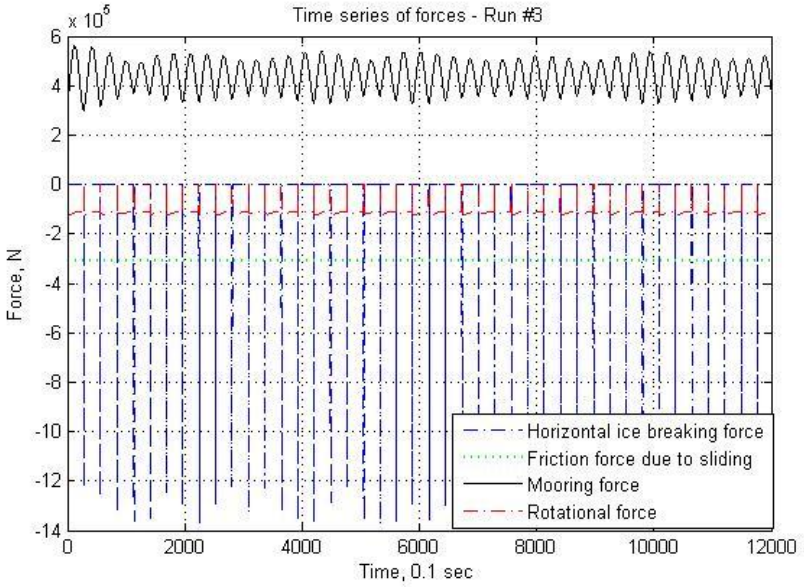

Figure 5.11: Simulation results – k=1125 kN/m, v=0.25 m/sec

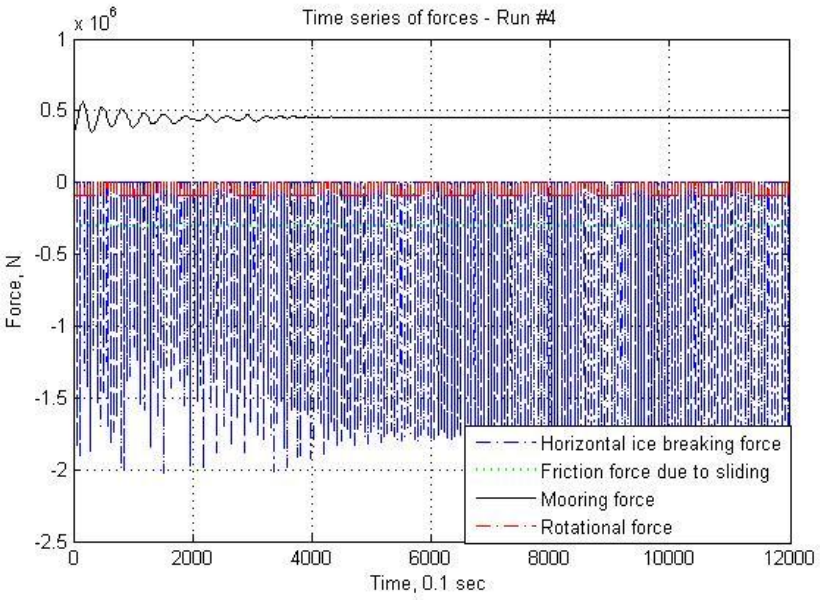

Figure 5.12: Simulation results – k=1125 kN/m, v=0.25 m/sec

The results of model tests are presented in Figure 5.13 and Figure 5.14.

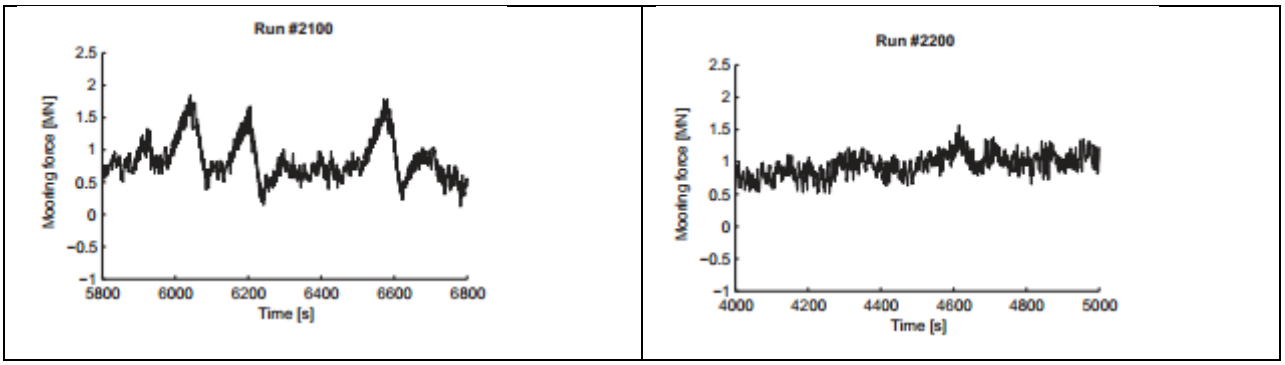

Figure 5.13: Data obtained from the model tests for mooring stiffness 250 kN/m: left - at velocity 0.05 m/sec, right – at velocity 0.25 m/sec (Aksnes, 2011)

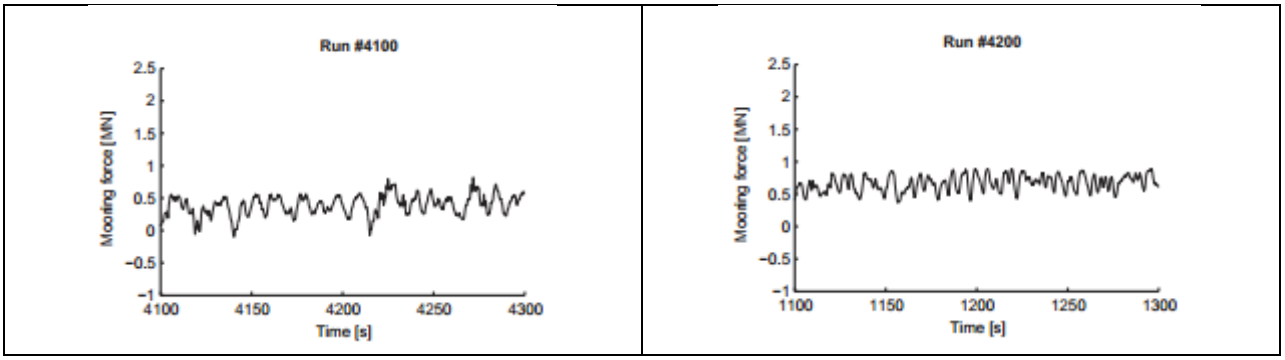

Figure 5.14: Data obtained from the model tests for mooring stiffness 1125 kN/m: left - at velocity 0.05 m/sec, right – at velocity 0.25 m/sec (Aksnes, 2011)

As can be seen from Figures 5.9 through 5.14 the magnitude of forces is predicted well.

CHAPTER 6: SUMMARY, CONCLUSION AND RECOMMENDATIONS FOR FURTHER WORK

6.1. Summary

The floating units for Arctic field developments are considered to be an attractive solution due to their operability in deep water areas and due to disconnection possibility. The extensive overview of the current experience of FPSO operations in ice environment is presented in Chapter 2 with the purpose to describe main design feature of floaters for ice conditions.

Particular problem of FPSO interaction with level ice has been addressed in the thesis. For this purpose two numerical models have been developed – the first one for an ice sheet bending and the second one for simulation of FPSO surge motion in level ice. The numerical model of ice sheet bending is based on the theory of thin plates. The problem was solved by means of finite difference method, "manually" implemented in MATLAB. The model has been intended to introduce a numerical tool for ice failure load calculation. However, the numerical tool developed can be widely used to solve other problems. The output parameters of the model, namely ice failure load and predicted failure mode were used as input parameters for the second numerical model devoted to FPSO surge motion in level ice.

6.2. Conclusions

- Floating production storage and offloading units are potentially capable to operate in harsh ice environments and represent an attractive solution for Arctic field developments;
- Numerical model of ice sheet bending developed in this thesis is considered to be a beneficial tool for investigation of ice-structure interaction;
- The numerical model developed allows prediction of failure mode and evaluation of ice failure load, which both are critical parameters for consideration of vessel's performance in ice.
- Comparison of the numerical model with full-scale data obtained for Bohai Bay in terms of failure mode prediction showed good agreement;
- The implementation of "nodal analysis" was proposed to evaluate contact width of an ice sheet with a structure;
- Numerical simulation of FPSO surge motion in level ice has shown good qualitative and satisfactory quantitative agreement;
- For the simulation of FPSO motion in level ice the use of velocity-dependent friction coefficient has been proposed;
- The phenomenon of increase of mooring loads at low ice drift velocity has been observed during numerical tests.

6.3. Recommendations for further work

- Investigation of fracture propagation in level ice in order to give recommendations on ice breaking length;
- The effect of increasing mooring loads at low ice drift speed should further be investigated.

LIST OF REFERENCES

1. Aksnes, V.Ø. (2011) *Experimental and Numerical Studies of Moored Ships in Level Ice*. Ph.D. thesis. Norwegian University of Science and Technology.
2. Allen, S. (2011) 10 Years of Sub Arctic Subsea Projects – Stepping Stones for Arctic Development. *In: Arctic Technology Conference*, Houston, Texas, USA, February 7-9, 2011. OTC 22115.
3. Blackerby, J. (2006) *Numerical Simulation of Dynamic Ice Forces on Offshore Structures*. New York: Clarkson University NSF REU.
4. Bonnemair, B., Jensen, A., Gudmestad, O.T., Lundamo, T. and Løset. S. (2007) Challenges related to station-keeping in ice. *In: 9th annual INSTOK Conference,* Houstan, Texas, March, 2007.
5. Edmond, C., Liferov, P. and Metge, M. (2011) Ice and Iceberg Management Plans for Shtokman Field. *In*: *Arctic Technology Conference*, Huston, Texas, USA, February 7-9, 2011.
6. Garratt, D.H. and Kry, P.R. (1978) Construction of artificial islands as Beaufort Sea drillinc platforms. *The Journal of Canadian Petroleum,* Montreal, April-June, 1978. Pp. 73-79.
7. Gudmestad, O.T., Løset, S., Alhimenko, A.I., Shkhinek, K.N., Tørum, A. and Jensen, A. (2007) *Engineering aspects related to Arctic offshore developments.* St. Petersburg: "LAN".
8. Gürtner, A. (2009) *Experimental and Numerical Investigations of Ice-Structure Interaction.* Ph.D. thesis. Norwegian University of Science and Technology.
9. Hnatiuk, J. and Felzien, E. E. (1985) Molikpaq: An Integrated Mobile Arctic Drilling Caisson. . 17th *Annual Offshore Technology Conference*, Houston, Texas, May 6-9, 1985. OTC 4940.
10. Hopkins, M.A. (2004) Discrete element modeling with dilated particles. *Engineering Computations*, Vol. 21, No. 2/3/4, pp. 422-430.
11. Hopkins, M.A. (1992) Numerical Simulation of Systems of Multitudinous Polygonal Blocks.
12. Hopkins, M.A. and Tuhkuri, J. (1999) Compression of floating ice fields. *Journal of geophysical research*, Vol. 104, No. C7, pp. 815–825.
13. Jirásek, M. and Bažant, Z.P. (1995) Macroscopic fracture characteristics of random particle systems. *International Journal of Fracture*, 69, pp. 201-228.
14. Jirásek, M. and Bažant, Z.P. (1995), Particle model for fracture and statistical micro-macro correlation of material constants. *In: Fracture Mechanics of Concrete Structures* (Proc" 2nd Int. Conf, on Fracture Mech, of Concrete and Concrete Structures (FraMCoS-2), held at ETH, Zurich), Freiburg, Germany, pp. 955-964.
15. Jirásek, M. and Bažant, Z.P. (1995) Particle model for quasibrittle fracture and application to sea ice. *Journal of engineering mechanics,* September 1995/1025.
16. Kärnä, T. and Jochmann, P. (2003) Field observations on ice failure modes. *In*: *POAC - International Conference*, Trondheim, Norway, 2003. Trondheim: Norwegian University of Science and Technology, pp. 839-848.
17. Level, G.V. and Kean, J.R. (2000) Harsh Environments FPSO Development for Terra Nova. *In: International Offshore and Polar Engineering Conference,* Seattle, USA, May 28-June 2, 2000.

18. Le Marechal , G., Anslot, P., Mravak, Z., Liferov, P. and Le Guennec, S. (2011) Design of a Floating Platform Hull for Arctic Conditions in the Barents Sea. *In*: *Arctic Technology Conference*, Huston, Texas, USA, February 7-9, 2011.
19. Li, F., Yue, Q. J., Shkhinek, K.N. and Karna, T. (2003) A Qualitative Analysis of Breaking Length of Sheet Ice Against Conical Structures. *In*: *POAC - International Conference*, Trondheim, Norway, 2003. Trondheim: Norwegian University of Science and Technology, pp. 293-304.
20. Løset, S. (2012) *Arctic Offshore Engineering lecture notes*. UNIS, Longyerbyen
21. Zhou, L., Riska, K., Moan, T., and Su, B. (2013) Numerical modeling of ice loads on an icebreaking tanker: Comparing simulations with model tests. *Cold region science and technology*, 87, pp. 33-46.
22. Zhou, L., Riska, K., von Bock und Polach, R., Moan, T., and Su, B (2013) Experiments on level ice loading on an icebreaking tanker with different ice drift angles. *Cold region science and technology*, 85, pp. 79-93.
23. Zhou, L., Su, B., Riska, K. and Moan, T. (2011) Numerical simulation of moored structure station keeping in level ice. *Cold region science and technology*, 71, pp.54-66.
24. Løset, S. (1994) Discrete element modelling of a broken ice field simulation of iec loads on a boom – part I. *Cold Regions Science and Technology*, 22, pp. 339-347.
25. Løset, S. (1994) Discrete element modelling of a broken ice field simulation of iec loads on a boom – part II. *Cold Regions Science and Technology*, 22, pp. 349-360.
26. Løset, S., Jensen, A. Gudmestad, O.T., Ravndal, O. and Eide, S.I. (2001) Model Testing of an Arctic Shuttle Barge System for Loading of Oil in Ice. *In: International Offshore and Polar Engineerhlg Conference*, Stavanger, Norway, June 17-22, 2001. Pp. 779-787.
27. Potapov, V.M., Blagovidov, L.B. and Minin V.V. (2001) Floating Production System for the Shtockmanovskoye Gas/Condensate Field. *In*: *11th International Offshore and Polar Engineering Conference*, Stavanger, Norway, June 17-22, 2001. pp. 315-318.
28. Sawamura, J., Tachibana, T., Tsuchiya, H. and Osawa, N. (2010) Numerical Investigation for the Bending Failure of Wedge-Shaped Floating Ice. *In*: *20th IAHR International Symposium on Ice*, Lahti, Finland, June 14-18, 2010.
29. Sedov, L.I. (1970) *Mechanics of continua* (in Russian). Vol. 1. Moscow: "Nauka".
30. Sedov, L.I. (1994) *Mechanics of continua* (in Russian). Vol. 2. 5th Ed. Moscow: "Nauka".
31. Srinivasan, N. (2011) Circular FPSO for arctic Deepwater. *In: Arctic Technology Conference*, Houston, Texas, USA, February 7-9, 2011. OTC 22136.
32. Su, B., Riska, K. and Moan, T. (2010) A numerical method for the prediction of ship performance in level ice. *Cold Regions Science and Technology*. Vol. 60, pp. 177-188.
33. Timco, G. W. (1984) Ice forces on structures: physical modeling techniques. *Second I.A.H.R. State-of-the-Art Report on Ice Forces on Structures*, Hamburg, Germany, 1984. Volume IV, Chapter 2.
34. Timoshenko, S. and Goodier, J.N. (1951) *Theory of elasticity*. New York: McGRAW-HILL BOOK COMPANY, Inc.
35. Timoshenko, S. and Woinowsky-Krieger, S. (1987) *Theory of plates and shells*. 2nd Ed. New York: McGRAW-HILL BOOK COMPANY
36. Todd, M.B. (1978) First offshore drilling in the Beaufort Sea. 10th *Annual Offshore Technology Conference*, Houston, Texas, May 8-11, 1978. OTC 3094.

37. Wang, C.H. (1996) *Introduction to Fracture Mechanics*. Melbourne Victoria: DSTO Aeronautical and Maritime Research Laboratory.
38. Zolotukhin, A. and Gavrilov, V. (2011) Russian Arctic Petroleum Resources: Challenges and Future Opportunities. . *In: Arctic Technology Conference*, Houston, Texas, USA, February 7-9, 2011. OTC 22062.

Appendix A – Case study of the numerical model of an ice sheet bending

Let us consider a case study of the application of the numerical model of an ice sheet bending. Parameters for the simulation run are listed in Table A.0.1: Parameters for case study.

Table A.0.1: Parameters for case study

Parameter	*Value*
Modulus of elasticity, E	5.4 GPa
Poisson's ratio, ν	0.3
Ice thickness, h	0.5 m
Contact width, b	5 m
External force, F	156 kN (upward)

The domain and boundary conditions are schematically illustrated in Figure A.1: Domain representation for the case study

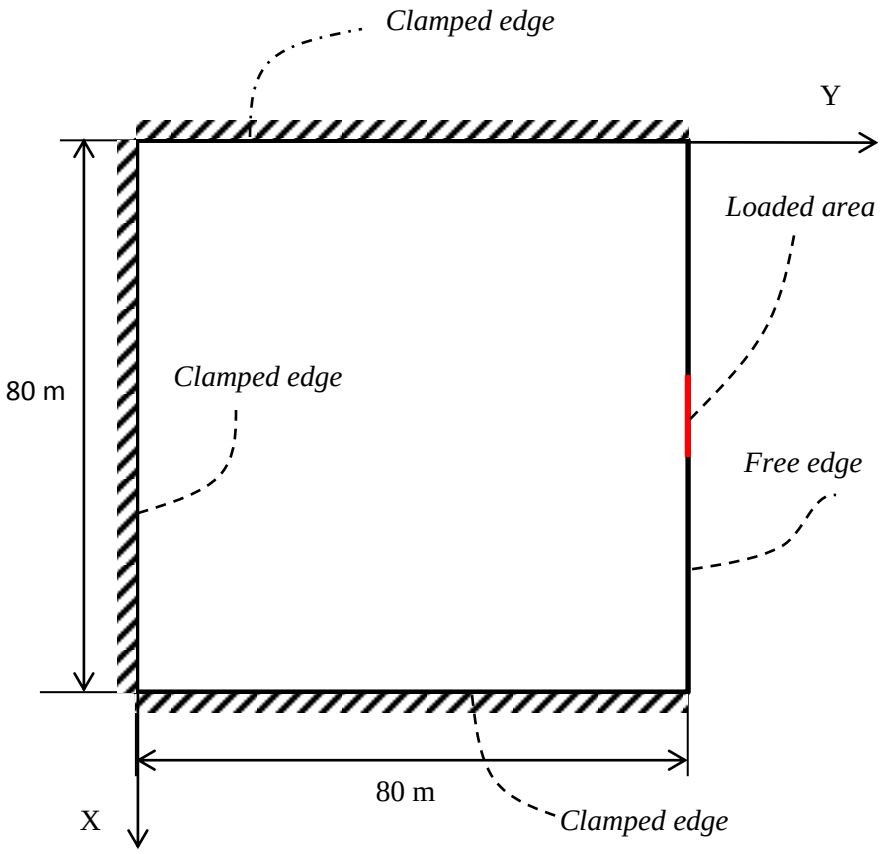

Figure A.1: Domain representation for the case study

Plate deflection

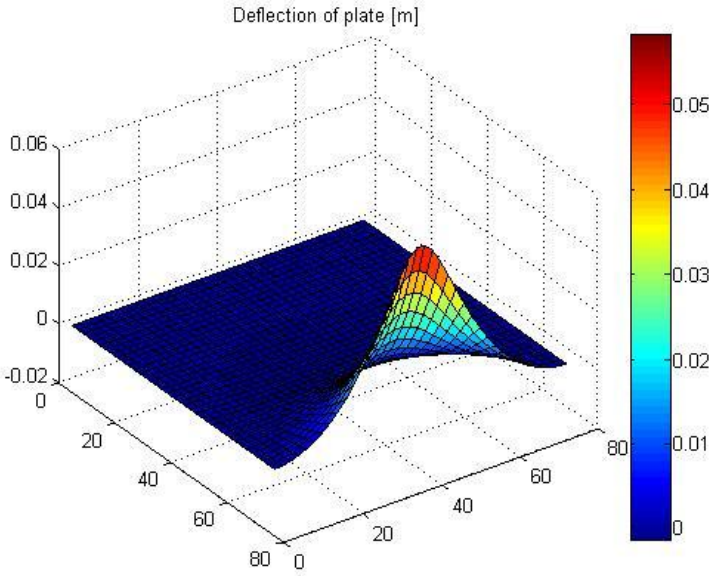

X displacements

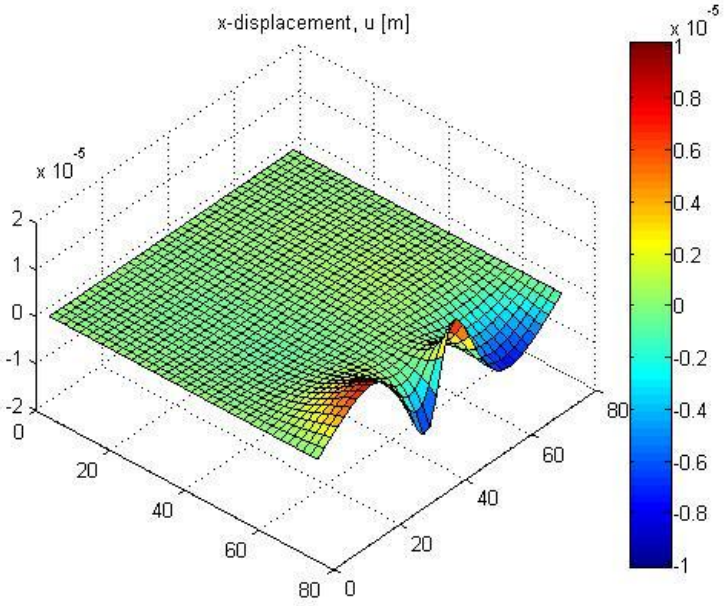

Y-displacements

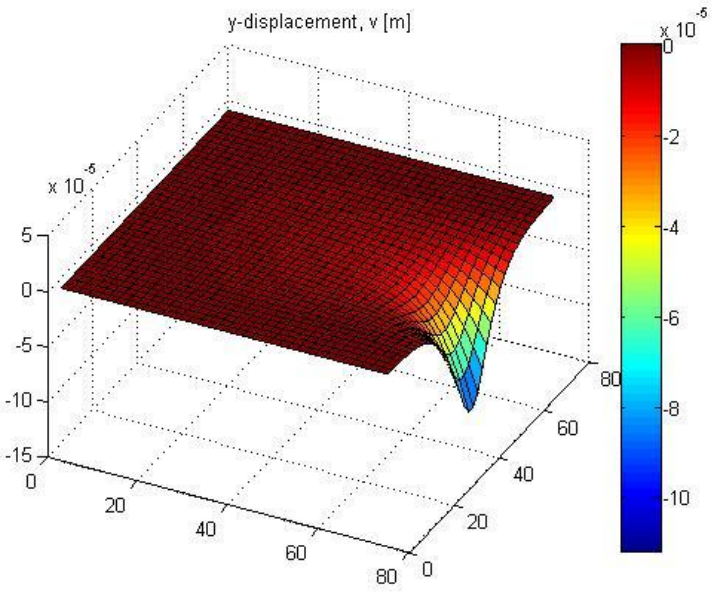

Bending moment in x-direction

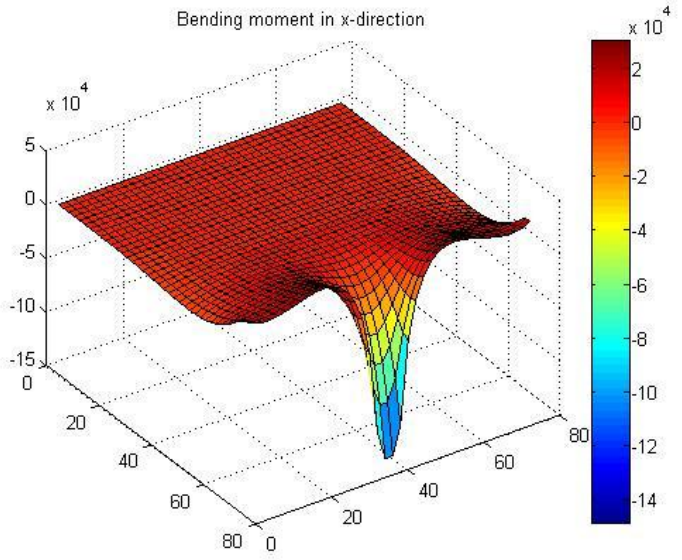

Bending moment in y-direction

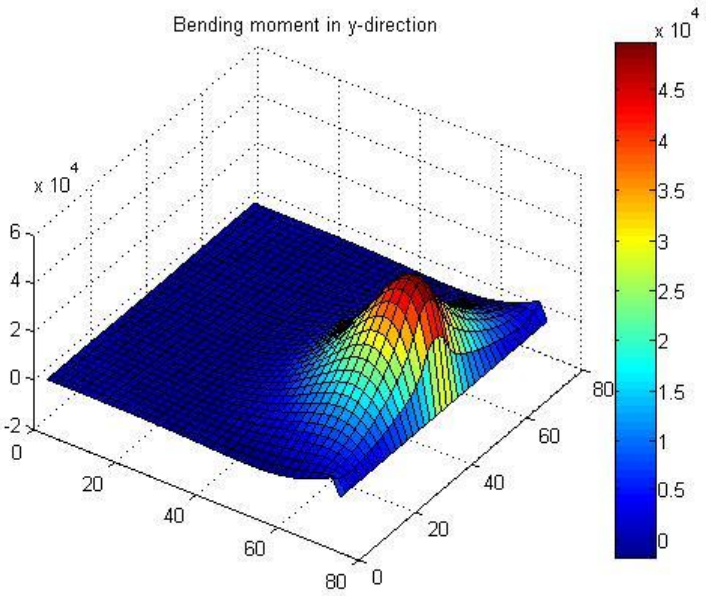

X-normal stress

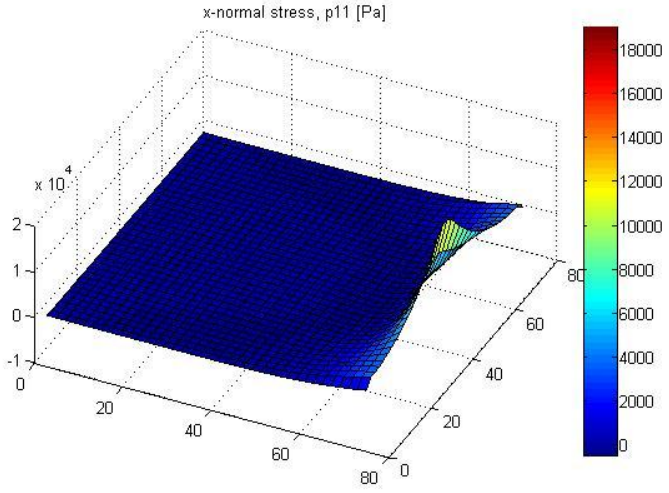

Y- normal stress

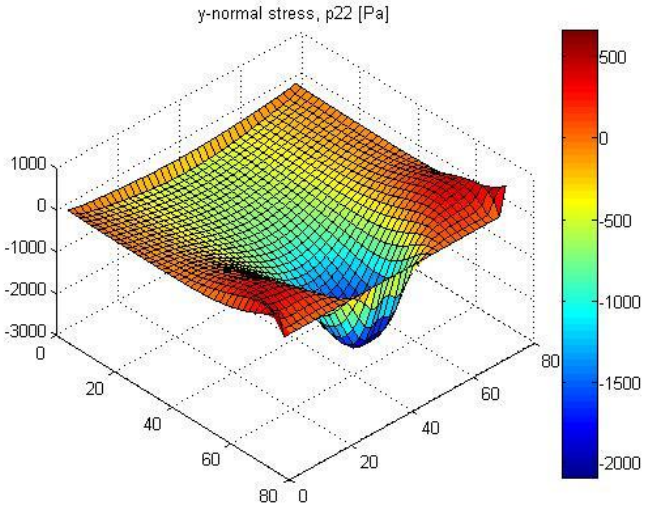

Von Mises stress at the bottom of plate